
Cenozoic Landscape Development in the Blue Mountains (SE Australia): Lithological and Tectonic Controls on Rifted Margin Morphology

Author(s): Peter van der Beek, Anna Pulford and Jean Braun

Source: *The Journal of Geology*, Vol. 109, No. 1 (January 2001), pp. 35-56

Published by: The University of Chicago Press

Stable URL: <https://www.jstor.org/stable/10.1086/317963>

JSTOR is a not-for-profit service that helps scholars, researchers, and students discover, use, and build upon a wide range of content in a trusted digital archive. We use information technology and tools to increase productivity and facilitate new forms of scholarship. For more information about JSTOR, please contact support@jstor.org.

Your use of the JSTOR archive indicates your acceptance of the Terms & Conditions of Use, available at <https://about.jstor.org/terms>



The University of Chicago Press is collaborating with JSTOR to digitize, preserve and extend access to *The Journal of Geology*

JSTOR

Cenozoic Landscape Development in the Blue Mountains (SE Australia): Lithological and Tectonic Controls on Rifted Margin Morphology

Peter van der Beek,¹ Anna Pulford,² and Jean Braun

Research School of Earth Sciences, Australian National University, Canberra ACT 0200, Australia
(e-mail: pvdbek@ujf-grenoble.fr)

ABSTRACT

Cenozoic landscape development on the southeastern Australian rifted margin, as recorded by mid-Tertiary basalt flows that preserve ancient landforms, is generally considered to be very slow. Eocene-Miocene basalts of the southeastern Australian highlands flowed down paleovalleys, indicating that landscape dissection was already well under way at the time of their eruption. Within the deeply incised Blue Mountains, however, Miocene basalts cap relatively flat hilltops, suggesting that most incision postdates their emplacement. We have studied the controls on these apparent lateral variations in Cenozoic landscape development using both field observations and numerical models. We have mapped the Blue Mountains basalts in detail to reconstruct the Miocene landscape and to quantify both the amount of subbasalt relief and postbasalt incision rates. New geochemical and K-Ar geochronological data indicate that most of the Blue Mountains basalts were derived from a common magma source and were erupted in a relatively short time span (20.1–14.5 Ma). Subbasalt relief is remarkably gentle; it does not exceed 100 m for any single basalt cap and is of the order of 200 m for the entire region. This contrasts sharply with a present-day relief of up to 700 m in major river gorges. By comparing the reconstructed mid-Miocene and present-day topographies, we estimate plateau lowering and river incision rates at <14 and ≤40 m m.yr.⁻¹, respectively. We explain the dramatic post-Miocene increase in regional relief by migration of major knickpoints up the river gorges, with retreat rates estimated at 800–1200 m m.yr.⁻¹. The kinematics of postbreakup knickpoint retreat thus play a fundamental role in modifying rifted-margin morphology. The Blue Mountains are bounded on the east by the Lapstone Structural Complex (LSC), a major faulted monocline that forms the present-day escarpment. Extrapolation of the estimated retreat rates suggests that knickpoints were initiated on this structure between 48 and 71 Ma. The Blue Mountains escarpment has been interpreted to result from either early Tertiary movement on the LSC or from passive denudation of previously tilted resistant sandstone at the monocline. We employ a numerical surface process model to explore these two hypotheses and conclude that, although lithological control cannot be excluded, early Cenozoic uplift, related to variations in intraplate stresses and/or magmatic underplating, appears to have been a major factor in shaping the anomalous morphology of the Blue Mountains region. This study reveals that significant lateral variation may exist in the morphologic development of rifted margins, and that local lithological and tectonic factors may interact in a complex manner to produce such variation.

Introduction

Over the last decade, the exposed onshore parts of rifted continental margins have been examined in order to understand the dynamics of their formation (e.g., Gilchrist and Summerfield 1994; Gallagher and

Brown 1997). The denudation history of these onshore regions, as recorded by thermochronological and geomorphological data, can be employed to decipher the history of rifted-margin uplift and denudation (e.g., Gallagher et al. 1994; van der Beek et al. 1995) as well as the sediment flux toward the offshore sedimentary basins (Brown et al. 1990; van Balen et al. 1995). Until recently, most studies that modeled these processes quantitatively considered rifted margins as fundamentally two-dimensional features, characterized by single “type” cross sec-

Manuscript received August 24, 1999; accepted August 15, 2000.

¹ Present address: Laboratoire de Géodynamique des Chaînes Alpines [CNRS UMR 5025], Université Joseph Fourier, BP 53, 38041 Grenoble Cedex, France.

² School of Earth Sciences, Victoria University of Wellington, P.O. Box 600, Wellington, New Zealand.

tions (e.g., Gilchrist and Summerfield 1990, 1994; Gallagher et al. 1994; van Balen et al. 1995; van der Beek et al. 1995). However, significant lateral variations may exist in rifted-margin morphology caused by laterally varying tectonic (uplift history) or lithological (preexisting geology) controls. As the uplift and denudation histories at rifted margins are intimately coupled to subsidence and sedimentation offshore, such lateral variations should be considered in studies of the structural and sedimentary evolution of the marginal basins.

The high-elevation rifted margin of southeastern Australia consists of an upland surface of low-to-medium relief known as the southeastern highlands. It is separated from a narrow, low-elevation coastal region by a prominent escarpment (Ollier 1982). The timing and mechanisms of the formation of the southeastern highlands have figured prominently in the literature on long-term landscape development and the morphotectonics of rifted continental margins (e.g., Summerfield 1991; Bishop and Goldrick 1999). Classical models for the evolution of the highlands followed almost exclusively "Davisian" thinking; their generally low relief was thought to result from peneplanation close to sea level, with Pleistocene uplift initiating the incision of valleys and landscape "rejuvenation" (e.g., Browne 1969).

Over the last two decades, the mapping and dating of widespread Cenozoic basalt remnants have provided significant new insights into the development of the highlands that have refuted their classical cyclical interpretation (e.g., Wellman and McDougall 1974; Young 1983; Bishop 1988). The basalts preserve Eocene-Miocene landscapes that show a relief comparable to the present day, demonstrating that the morphology of the highlands is of much greater antiquity than previously assumed (e.g., Bishop et al. 1985; Taylor et al. 1985, 1990; Young and McDougall 1985, 1993). These studies pushed back the conceivable onset of highlands uplift to pre-Cenozoic times and stimulated new tectonic models for their formation. At present, the highlands are generally thought to result from regional uplift and/or baselevel drops related to mid-Cretaceous rifting and breakup of the Tasman Sea (cf. reviews by Bishop and Goldrick 1999; van der Beek and Braun 1999). Most studies have either implicitly or explicitly assumed morphological unity of the southeastern highlands so that the entire highland belt could be described by a single evolutionary model. However, significant lateral variations in the highlands' morphology cast doubt on such a concept (Bishop 1988; van der Beek and Braun 1998; Bishop and Goldrick 1999).

The Blue Mountains of central New South Wales (figs. 1–3) are a highlands region that developed on Permo-Triassic sediments of the Sydney Basin rather than on Paleozoic basement. They show conspicuous morphological anomalies with respect to surrounding highlands sections. The escarpment forming the eastern margin of the highlands contains a large embayment in the central Sydney Basin, where it is located nearly 100 km inland, whereas to the north and south of the basin it lies within 30 km of the coast (fig. 1, *inset*). River profiles within the Sydney Basin are graded up to a steep reach in their headwaters and appear "pinned" against the drainage divide, in contrast to rivers flowing over Paleozoic basement that are characterized by major knickpoints (Nott et al. 1996; Seidl et al. 1996; van der Beek and Braun 1999). Stratigraphic patterns on the continental shelf off southeastern Australia also vary laterally. Most of the New South Wales margin is characterized by a thin offlapping Neogene sedimentary wedge, but offshore Sydney this wedge is unconformably overlain by an upper unit of onlapping strata (Davies 1975), suggesting regional variations in accommodation space and/or sediment flux from the highlands (van Balen et al. 1995). Finally, the geomorphic history preserved by basalt remnants in the Blue Mountains may differ from that elsewhere in the highlands. Most of the Paleocene-Miocene basalts mapped previously in the southeastern highlands flowed down paleovalleys, indicating that river incision was already well advanced at the time of their eruption (e.g., Bishop et al. 1985; Taylor et al. 1990; Young and McDougall 1993). In contrast, the Blue Mountains basalts cap relatively flat hilltops (cf. fig. 2), suggesting that they may be remnants of an initially continuous subhorizontal sheet and predate river incision (Carne 1908; Wellman 1979).

These apparent differences in the mode of landscape development, which have hitherto not been examined in detail, may be related to lateral variations in lithological or tectonic controls on the evolution of the southeast Australian rifted margin. In this article, we analyze basalt outcrops in the western Blue Mountains to reconstruct the pre-basaltic topography. We use new geochemical and K-Ar age data from these basalts to correlate them and to assess the likelihood that they indeed once formed a continuous cover. Using these data, we reconstruct the region's Cenozoic geomorphic history and calculate rates of upland lowering, river incision, and knickpoint retreat, comparing our findings with those from elsewhere in the highlands. Finally, we present numerical surface process

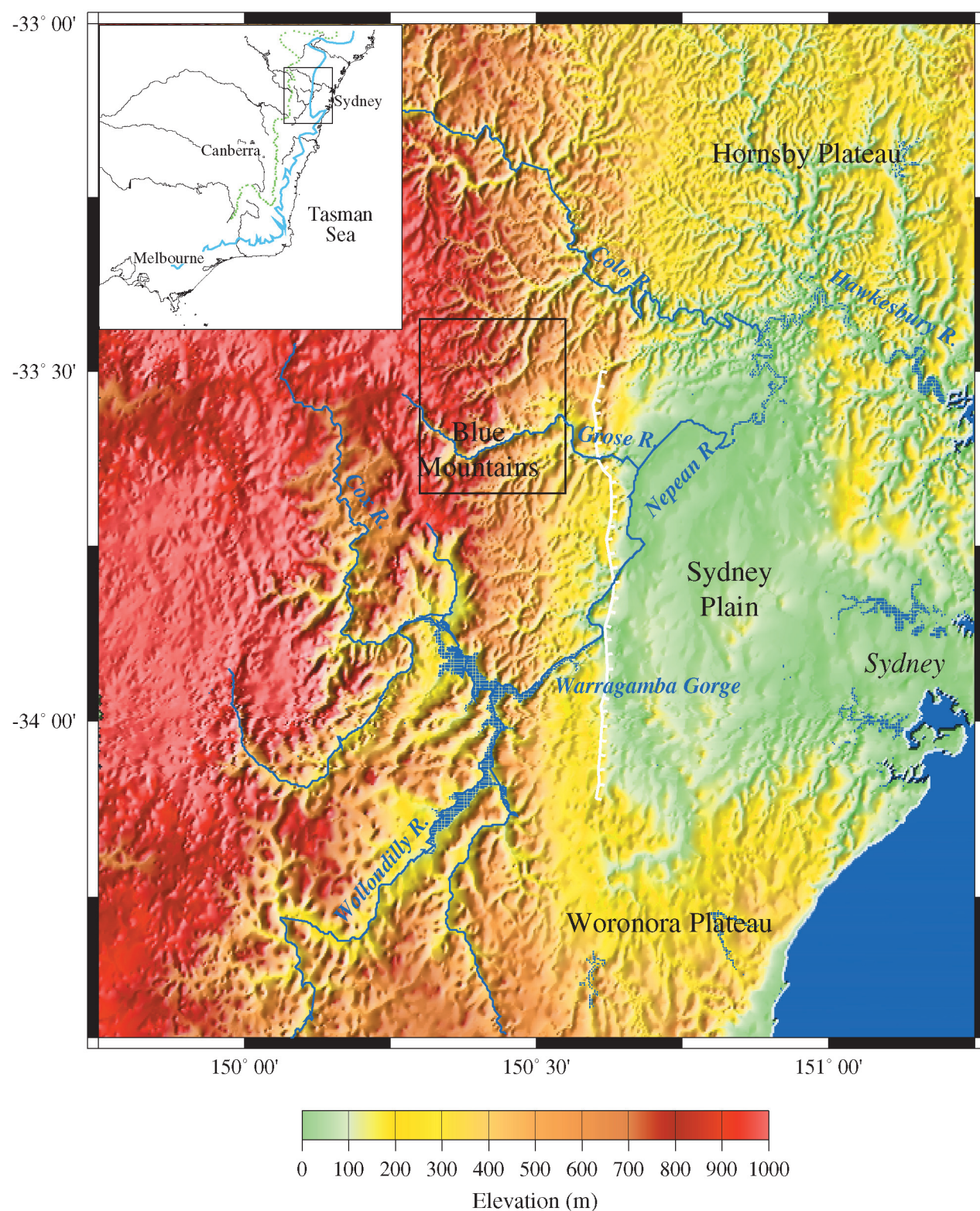


Figure 1. Shaded relief map of the Blue Mountains and surrounding regions, created from the AUSLIG 9 arc-second DEM. Box indicates the field study area. Thick line with fault notation denotes the Lapstone Structural Complex. Inset shows the location within southeastern Australia, as well as major rivers (thin black lines), the top of the escarpment (thick blue line), and continental drainage divide (dotted green line).

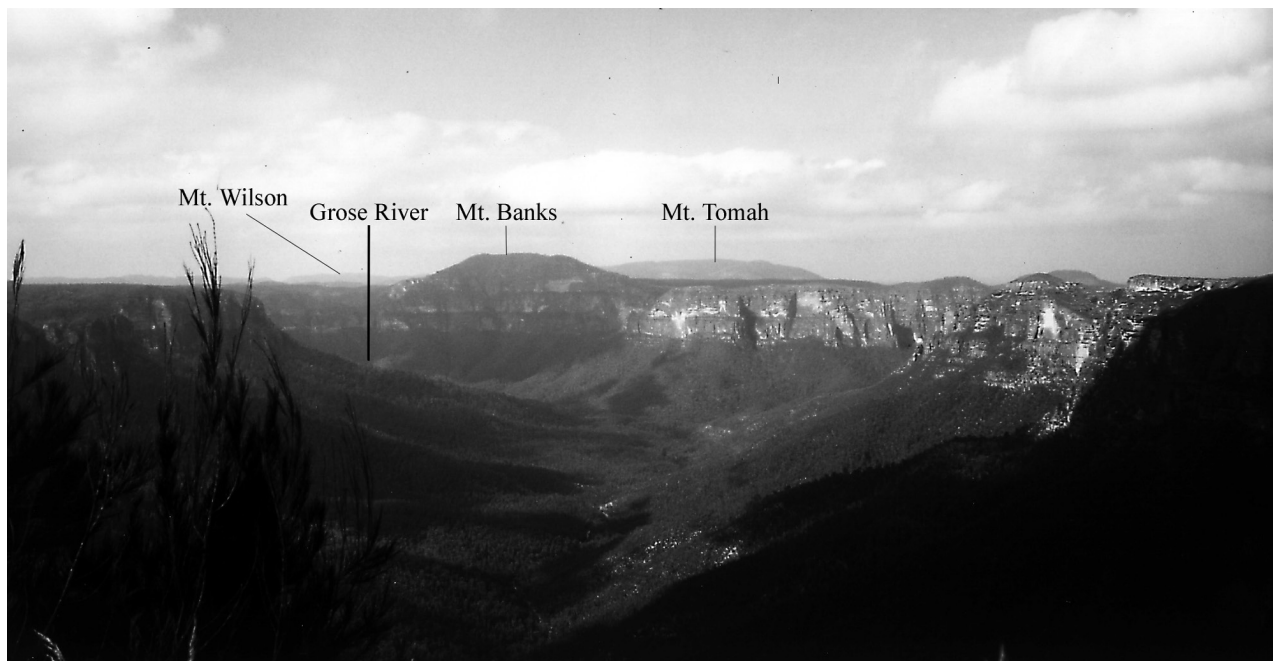


Figure 2. View of the Grose River gorge and Mt. Banks from Evans Lookout (AMG Reference 522754, looking NE—cf. fig. 4 for location). The valley in the foreground is Govetts Creek. Mt. Wilson and Mt. Tomah can be seen on the horizon to the left and right of Mt. Banks, respectively. Note near-horizontal contact between light-colored, cliff-forming Hawkesbury and Narrabeen sandstones and Miocene basalts (dark hilltop) on Mt. Banks.

model simulations of landform evolution in the Blue Mountains to quantify the relative importance of lithological versus tectonic controls on this evolution.

Regional Setting

The Blue Mountains consist of relatively flat upland plateaus, 800–1000 m high, incised by dendritic gorges that create several hundred meters of relief (figs. 1, 2). Drainage is collected by three major rivers, the Colo, Grose, and Cox, that all flow into the Nepean River. The Nepean flows northward, parallel to the Blue Mountains escarpment, for ~100 km before bending sharply eastward, becoming the Hawkesbury River, and cutting a gorge through the low-elevation Hornsby Plateau to reach the Tasman Sea (fig. 1).

The Blue Mountains form part of the Sydney Basin (fig. 3), a Permo-Triassic foreland basin that formed during collision of the Lachlan and New England tectonic blocks (cf. Veevers et al. 1994). Maximum sediment thickness is ~5 km at its northeastern border, where the basin is overthrust by the New England Fold Belt. To the southwest,

Permian and Lower Triassic strata onlap basement. Permian sediments include the shallow-marine Shoalhaven Group and the deltaic Illawarra Coal Measures. The Triassic succession is dominated by the Narrabeen and Hawkesbury fluvial sandstone groups. The uppermost preserved unit of the Sydney Basin consists of the upper Triassic lacustrine Wianamatta Shale, but a significant amount of overlying sediments must have been stripped by late Mesozoic-Cenozoic erosion (Middleton 1993; O'Sullivan et al. 1996a).

Sydney Basin strata show little deformation except for tilting in north-south trending monoclines, the largest of which is the Lapstone Structural Complex (LSC). This faulted monocline coincides with the escarpment separating the Blue Mountains plateau from the low-lying coastal plain and shows some 500 m of structural relief (Pickett and Bishop 1992). Movement on the monocline was accompanied by normal faulting on the west-dipping Kurrajong fault and by reverse faulting further to the south on the east-dipping Glenbrook and Nepean faults (fig. 3). The LSC is a long-lived tectonic feature with associated gravity and magnetic signatures that identify it as a crustal-scale structure

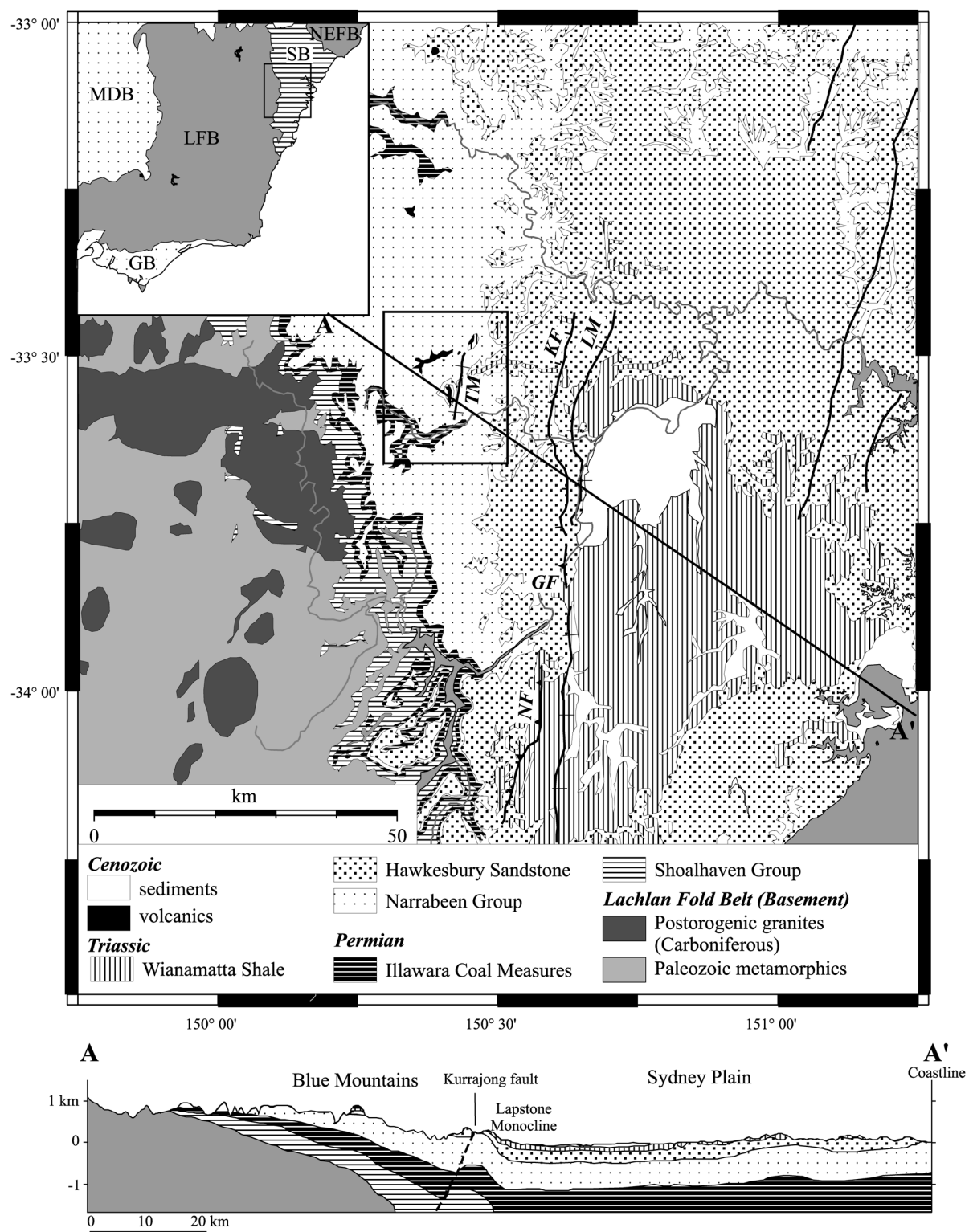


Figure 3. Simplified geological map and cross section of the Blue Mountains and surrounding regions, modified from Bryan (1966). Box indicates location of figure 4. Inset shows the tectonic setting of the Sydney Basin (SB) within southeastern Australia. GB, Gippsland Basin; MDB, Murray-Darling Basin; LFB, Lachlan Fold Belt; NEFB, New England Fold Belt; GF, Glenbrook Fault; KF, Kurrajong Fault; NF, Nepean Fault; LM, Lapstone Monocline; TM, Tomah Monocline.

(Branagan et al. 1976; Branagan and Pedram 1990). The smaller Tomah Monocline (Goldberry 1972) lies parallel to the Lapstone structure about 20 km farther inland. The monoclines were active during sedimentation, as the sedimentary units thicken eastward across them (Bryan 1966; Goldberry 1972).

The post-Triassic tectonic history of the LSC and the related uplift history of the Blue Mountains are, however, controversial. The classical interpretation (e.g., Branagan and Pedram 1990) is that the Blue Mountains were uplifted during the early Cenozoic as a result of renewed activity of the LSC and that the Blue Mountains escarpment thus has a tectonic origin. Pickett and Bishop (1992), in contrast, suggest that the escarpment formed by passive exhumation of the tilted resistant Hawkesbury and Narrabeen sandstones within the monocline, arguing for a purely lithological control on the escarpment location. A paleomagnetic study by Bishop et al. (1982) indicated that movement on the LSC had ceased by the Miocene, whereas Schmidt et al. (1995) presented paleomagnetic results that support post-mid-Cretaceous movement on the structure. Taken together, these data roughly constrain the latest movement on the LSC to the Paleogene.

Although lithological control on the Blue Mountains morphology is thus controversial on a regional scale, its role can be well demonstrated on more local scales (Branagan et al. 1976; Young and Nanson 1983). The flatness of the Blue Mountains plateaus appears to be controlled by horizontal bedding in the massive and resistant Triassic sandstones. Gorge morphology is also lithologically controlled; smaller rivers that have not incised into Permian sediments form V-shaped gorges with rectilinear mantled sidewalls, similar to gorges in Paleozoic basement north and south of our study area (Nott et al. 1996; Seidl et al. 1996; Weissel and Seidl 1998). In contrast, deep incision by the Grose River has exposed less resistant Permian strata in its upper reach (fig. 3), resulting in a wide and deep gorge topped by vertical cliffs where Triassic sandstones are exposed (fig. 2). Gorge widening and sidewall steepening are caused by undercutting of the sandstones by sapping, once the riverbed reaches the softer Permian sediments (e.g., Branagan et al. 1976).

Blue Mountains Basalts

Field Occurrence. Scattered basalt outcrops occur over approximately 140 km² within the Blue Mountains, about 70 km northwest of Sydney. One

of us has mapped the basalt in detail (Pulford 1997), with particular emphasis on the large discontinuous outcrop that caps Mts. Wilson, Irvine, and Tootie (fig. 4). The Mt. Tomah basalt was previously mapped by Pickett (1984); his map is reproduced as part of figure 4. The basalt contact was followed where possible and plotted on 1 : 25,000 topographic maps; elevations were cross-checked using an altimeter calibrated on geodetic monuments. The base of the basalts is often obscured by abundant vegetation or rock slides. Where the contact could not be followed, it was interpolated from nearby contacts or inferred from small terraces or changes in slope gradient. We estimate the horizontal accuracy of the mapped basalt contact to be between 10 and 100 m, depending on local outcrop conditions, and the uncertainty in vertical position of the contact to be <20 m.

The basalt disconformably overlies Sydney Basin sediments; the western and central outcrops occur directly on Hawkesbury or Narrabeen Group sandstones, whereas the easternmost caps have preserved a veneer of Wianamatta Shale. Basalt caps are generally about 50–60 m thick but reach 140 m on Mt. Tomah (Pickett 1984). Variations in columnar jointing characteristics, as well as intrabasaltic terraces, suggest that the caps are made up of several flows, with a maximum flow thickness of 20 m. At least three flows can be distinguished on Mt. Tomah, three on Mt. Banks, and at least two on Mt. Wilson. However, generally poor outcrop conditions prevent the construction of a basalt stratigraphy and the correlation of flows between outcrops. In contrast to other basalts in southeastern Australia (e.g., Bishop et al. 1985; Nott 1992; Young and McDougall 1993), no subbasaltic stream sediments were encountered.

The subbasaltic contact appears to form a gently northeast-dipping surface. The contact lies at around 1000 m at the west end of Mt. Wilson but only at 750 m at Mt. Tootie. Within a single outcrop, maximum subbasaltic relief is on the order of 50–80 m on Mts. Wilson and Tomah. At first sight, the outcrop pattern on Mt. Wilson appears to resemble a paleochannel with its tributaries. However, the basalt contact slopes away from the central axis of the cap, which would correspond to the main channel. We therefore interpret the Mt. Wilson outcrops as representing a basalt flow on a ridge, with a probable flow direction to the east. The basalts on Mt. Tomah, in contrast, appear to have flowed down a 50-m-deep paleochannel to the west (Pickett 1984). The base of the basalt on Mt. Irvine slopes over 5° to the east over a wide area, suggesting flow of the basalt down a hillslope.

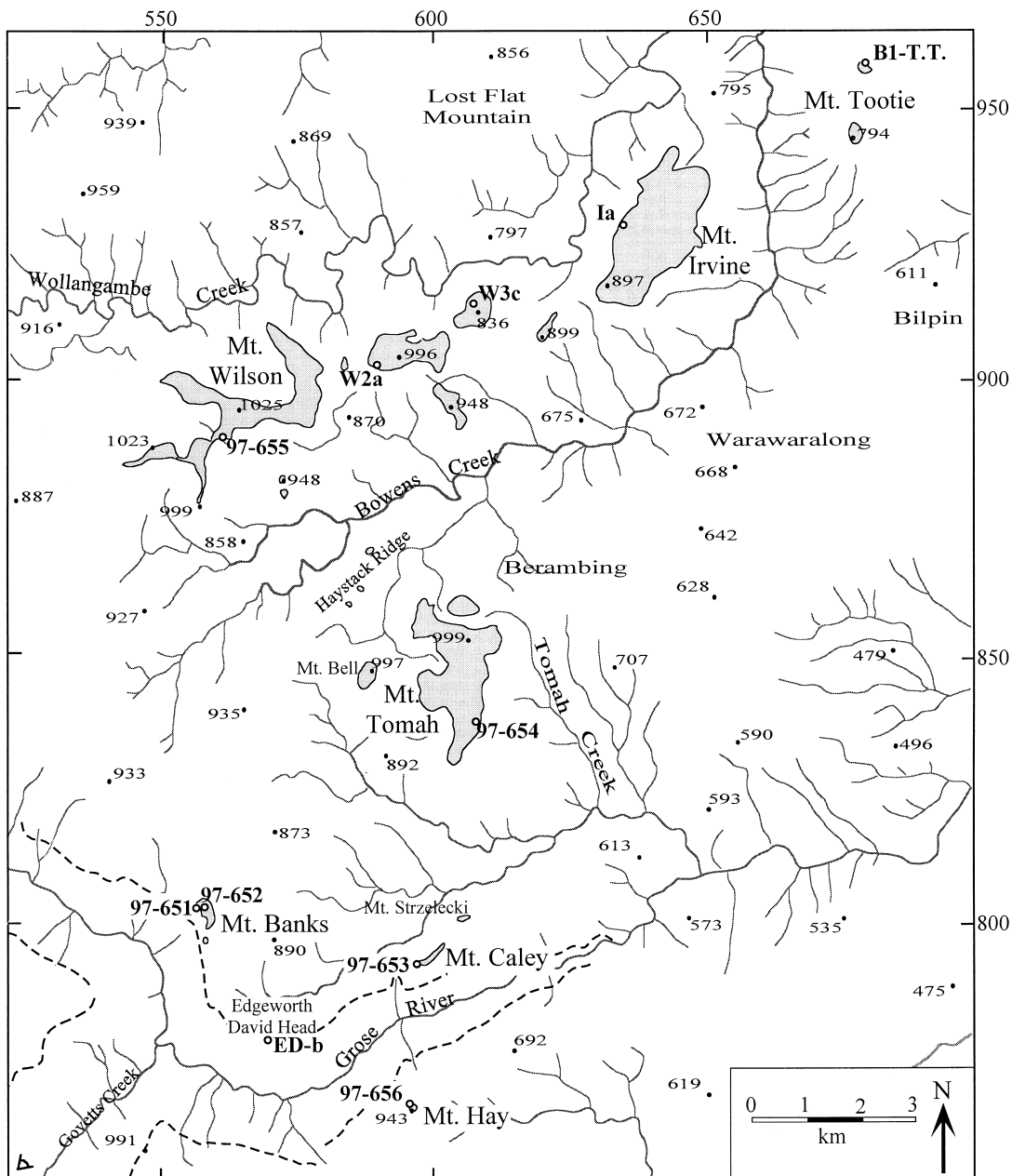


Figure 4. Detailed map of basalt outcrops within the study area showing sample locations for geochemical and K-Ar analyses. Base map shows drainage and selected hilltop elevations, as well as villages. Grid scale is the Australian map grid (AMG) reference of 1 : 50,000 topographic series, sheets 8930-1-N (Mt. Wilson), 8931-2-S (Wollangambe), and 9031-3-S (Mountain Lagoon). Thick dashed lines in SW corner of map indicate cliffs around upper Grose River. "Eye" symbol in lower left corner indicates viewpoint of figure 2.

The subbasaltic surface below the southern outcrops appears to be extremely flat. On Mt. Banks, for instance, the sandstone-basalt contact shows <10-m variation over the 1-km-wide outcrop (fig. 2). The Mt. Caley basalt crops out at 790–840 m, 100 m below Mt. Hay (the only basalt outcrop south of the Grose River gorge) and 200 m below Mt.

Banks, suggesting that a paleo-Grose valley may have existed before eruption of the basalts. Finally, the basalt outcrop at Edgeworth David Head is distinctively oval in shape and lies below the surrounding sandstone. The basalt-sandstone contact is very abrupt and consists of a 1.5-m-high sandstone cliff, suggesting that this outcrop represents

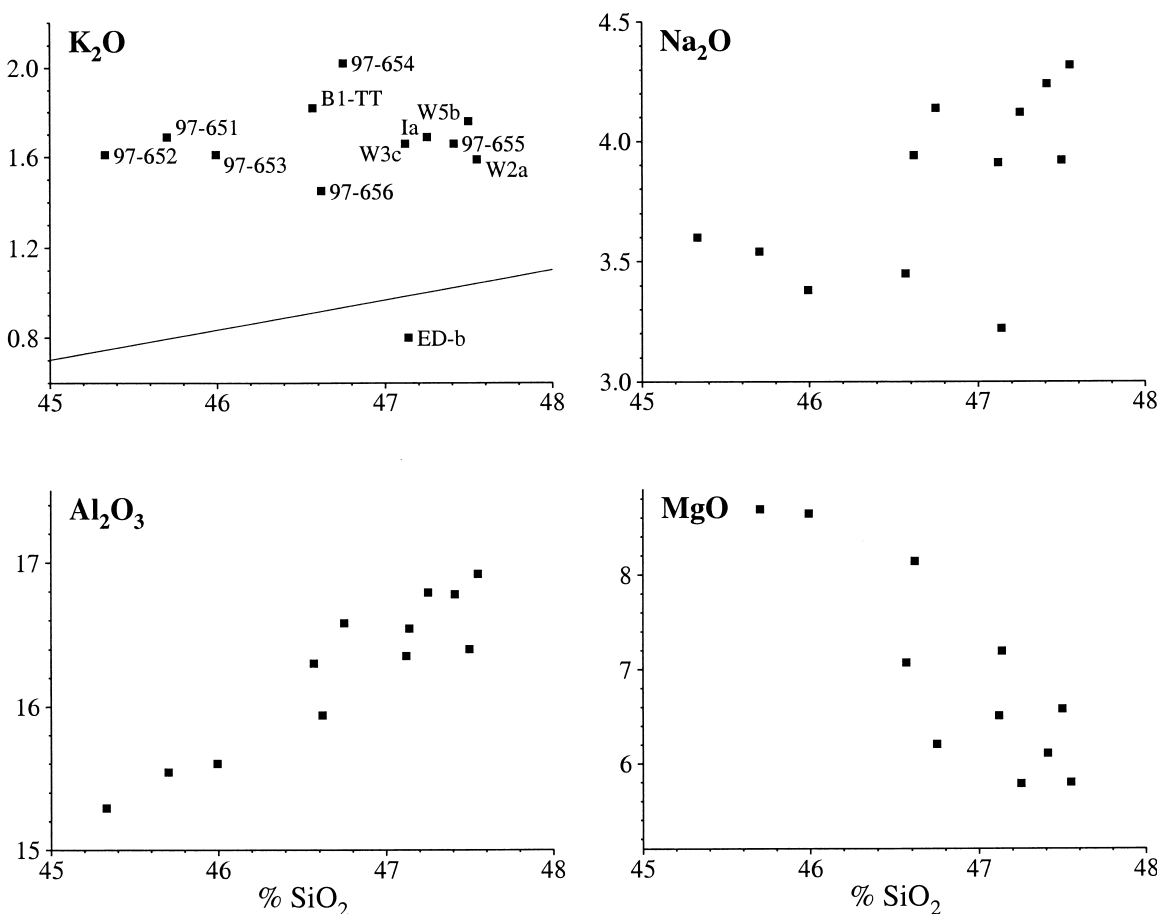


Figure 5. Major element (Harker) diagrams for the analyzed basalt samples. Samples are identified in the K_2O - SiO_2 plot (upper left), which also shows the boundary between alkaline and subalkaline fields after Middlemost (1975).

a feeder pipe. A magnetic traverse of the area, however, did not provide a conclusive geometry of the basalt fill (J. Pickett, pers. comm., 1997).

In conclusion, the subbasaltic topography shows much lower relief than the present-day topography. Maximum subbasaltic local relief is on the order of 200 m, and mostly is <100 m, whereas present-day local relief attains 700 m.

Geochemistry. The petrography and geochemistry of the basalts was studied from thin sections and XRF analyses and is described in detail in the appendix (available from *The Journal of Geology* office free of charge upon request). Both mineralogy and major-element compositions vary little between samples. All are alkali olivine basalts except the sample from Edgeworth David Head, which is a transitional subalkali basalt. Major elements vary consistently between the analyzed samples, suggesting a common derivation from a fractionating magma source (fig. 5). In general, variations in

trace-element geochemistry between the samples are small (fig. 6), although noticeable spread occurs for the less incompatible elements. Most of the northern samples, notably W2a (Mt. Wilson), Ia (Mt. Irvine), and 97-654 (Mt. Tomah), show a significant depletion in these elements, whereas the southern samples 97-651 and 97-652 (Mt. Banks), 97-653 (Mt. Caley), and 97-656 (Mt. Hay) appear enriched. Sample ED-b (Edgeworth David Head) shows negative anomalies for all of the highly incompatible elements. These results, in common with the major elements, suggest a fractionation trend evolving from south to north.

To test the hypothesis of fractionation from a common source, we examined Ni and Zr concentrations. These elements behave inversely during fractionation, are relatively insoluble, and have a low probability of contamination. Therefore, in samples derived from a simple fractionating sys-

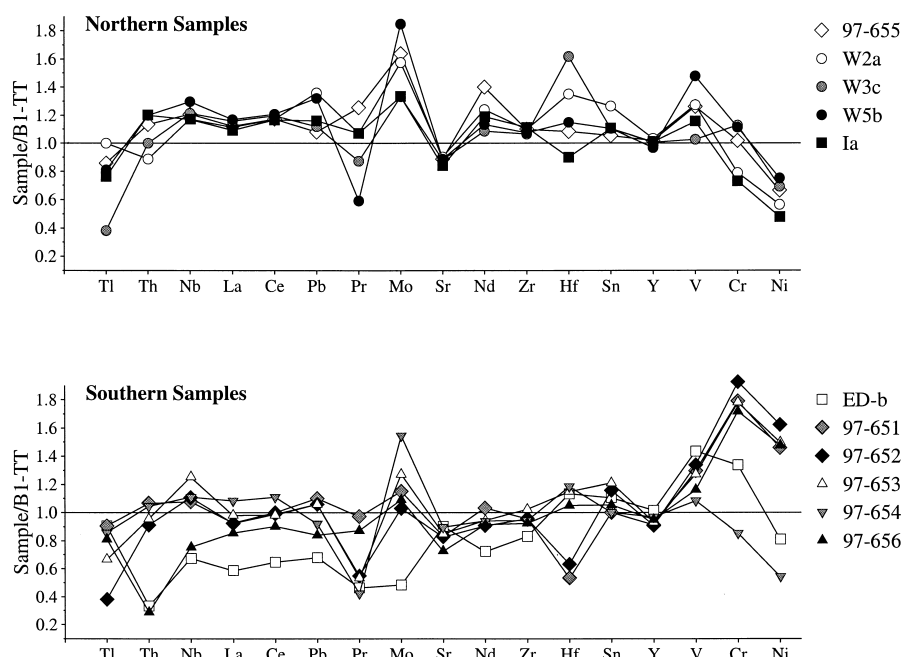


Figure 6. Selected trace-element spider diagrams for Blue Mountains basalt samples. Trace-element concentrations are plotted normalized to those encountered in B1-TT, which is the sample with the most “average” composition. Top panel shows results from northern samples (Mts. Wilson, Irving, and Tootie); lower panel shows central and southern samples (Mts. Tomah, Banks, Caley, Hay, and Edgeworth David Head).

tem, these elements should be strongly negatively correlated (e.g., Wilson 1989). The Ni versus Zr plot (fig. 7) indeed shows such a trend, with the northern samples clustering toward the highly fractionated end of the plot, the southern ones toward the less fractionated end, and Mt. Tootie (B1-TT) in between. Three samples fall significantly off this fractionation trend: ED-b (Edgeworth David Head), 97-654 (Mt. Tomah), and, to a lesser extent, 97-653 (Mt. Caley). The former two also show conspicuous differences in other major and trace elements (cf. appendix).

We conclude from the geochemical analysis that most of the basalts were derived from a single fractionating magma source. The Edgeworth David Head sample shows significant anomalies in both major- and trace-element compositions. Since we interpret this outcrop to be a pipe, the sample may represent the subsequent evolution of the magma source related to later eruptions, the products of which have been removed by erosion. The samples from Mt. Tomah (and possibly Mt. Caley) are also sufficiently different in composition to suggest that they have been derived from a different source.

K-Ar Ages. Basalts from Mt. Tomah and Mt. Wilson have been dated previously by Wellman and McDougall (1974) at 15.0 ± 0.4 Ma and $16.7 \pm$

0.4 to 18.3 ± 0.7 Ma, respectively, when recalculated using the Steiger and Jäger (1977) decay constants. However, basalts of very different ages occur in close proximity to each other elsewhere in the highlands (e.g., Bishop et al. 1985; Young and McDougall 1985) so that these ages cannot be extrapolated a priori to the other basalt caps. We have therefore selected six additional samples for K-Ar age determination based on suitability for dating

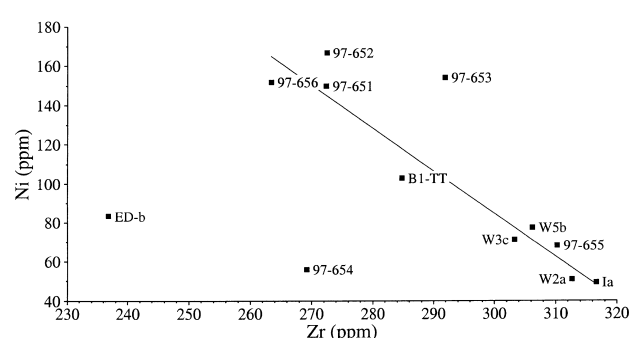


Figure 7. Ni versus Zr fractionation diagram. Continuous line indicates best-fit linear regression on all samples except ED-b (Edgeworth David Head), 97-654 (Mt. Tomah), and 97-653 (Mt. Caley).

as well as geographical spread (fig. 4). The dating techniques are similar to those used previously to date southeastern Australian basalts (e.g., Bishop et al. 1985; Young and McDougall 1985, 1993; Nott et al. 1996) and are described in the appendix.

K-Ar ages are given in table 1; uncertainties are quoted as the 1σ analytical error. All samples are Early to Middle Miocene in age. The oldest age is from Mt. Caley (97-653) at 20.4 ± 0.2 Ma. The Mt. Wilson sample (97-655) has an age of 17.9 ± 0.2 Ma, consistent with the older of the ages reported by Wellman and McDougall (1974). The lower sample from Mt. Banks (97-651) and the sample from Mt. Hay (97-656) produce similar ages of 15.0 ± 0.2 to 15.4 ± 0.2 Ma. The age of our Mt. Tomah sample (97-654) overlaps that of Wellman and McDougall (1974) at 14.2 ± 0.2 Ma and is similar to the age found at the top of Mt. Banks (97-652; 14.2 ± 0.2 Ma).

Replicate measurements were done on both Mt. Banks samples because of their different apparent ages. The replicate measurements were fully consistent with the first determinations so that the age difference between the base and the top of the basalt cap is real. This indicates at least two flows on Mt. Banks, consistent with the field data. Similarly, the age differences on Mt. Wilson suggest multiple eruptive episodes, spanning locally some 3 m.yr. In general, the sample quality, as well as the consistency of results, both internally within our study and in comparison with the results of Wellman and McDougall (1974), suggests minimal argon loss and provides confidence in interpreting our age data.

There is no trend between the ages and altitudes of the samples, as would be expected in the case of active landscape downcutting (leading to a negative correlation) or filling (positive correlation). The Mt. Caley sample, however, represents the lowest and also the oldest basalt in the area. This suggests that a precursor of the Grose River valley existed at 20

Ma, that this valley was 100–200 m deep, and that it may have been partially filled by basalt flows between 20 and 14 Ma. Significantly, the similarities in both geochemistry and age between the (lower) Mt. Banks and Mt. Hay basalts suggest that they were erupted during a common volcanic event. Because these outcrops occur north and south of the Grose River gorge, respectively, this result strongly suggests that incision of the gorge locally postdates the basalts.

Implications for Landscape Development

The geochemical and geochronological data indicate that the Blue Mountains basalts erupted over a limited time span (~ 20 –14 Ma) and that most of them were derived from a common magma source. A first eruptive event at ~ 20 Ma, sampled at Mt. Caley, appears to have filled a paleovalley. A subsequent phase at around 17–18 Ma was centered on Mt. Wilson; basalts with a similar parent magma erupted around 15–14 Ma in the central and southern parts of the study area. This phase appears to be the most widespread and, importantly, left remnants both north and south of the Grose River gorge. Finally, a more local eruption may have formed the Mt. Tomah basalt at around 14 Ma.

Because of the broad similarities in both age and geochemistry for most of the basalts, we assume that the mapped basalt contacts represent a single Middle Miocene paleotopographic surface. We will attempt to reconstruct this paleosurface by interpolation and use it to quantify differences between Miocene and present-day relief as well as post-Middle Miocene rates of plateau lowering and fluvial incision.

Paleotopographic Modeling. We have recorded the position and altitude of the basalt base at 662 sites in the field area and have used these data to construct a map of the Miocene topography by nu-

Table 1. K-Ar Age Measurements on Whole-Rock Basalt Samples from the Blue Mountains

Sample no.	K (wt %)	Rad. ^{40}Ar (10^{-11} mol/g)	Rad. $^{40}\text{Ar}/\text{Total Ar}$ (%)	Age $\pm 1\sigma$ (Ma)	Altitude (m)	Map grid reference ^a
97-651 (1)	1.460, 1.431	3.79	67.2	$15.1 \pm .2$	1030	556,804
97-651 (2)		3.80	62.6	$15.0 \pm .2$		
97-652 (1)	1.413, 1.434	3.50	52.7	$14.1 \pm .2$	1045	556,804
97-652 (2)		3.52	47.0	$14.2 \pm .2$		
97-653	1.178, 1.171	4.19	63.2	$20.4 \pm .2$	790–830 ^b	597,794
97-654	1.746, 1.753	4.34	44.3	$14.2 \pm .2$	945	607,837
97-655	1.407, 1.413	4.40	64.0	$17.9 \pm .2$	950	562,898
97-656	1.254, 1.264	3.38	62.4	$15.4 \pm .2$	935	596,767

Note. Constants used: $^{40}\text{K}/\text{K} = 1.167 \times 10^{-4}$; $\lambda_e = 5.811 \times 10^{-11} \text{ yr}^{-1}$; $\lambda_\beta = 4.962 \times 10^{-10} \text{ yr}^{-1}$.

^a Australian map grid reference on sheet 8930-1-N [Mt. Wilson 1 : 50,000].

^b Sample collected in rock slide at 790 m; summit of Mt. Caley at 830 m.

merical interpolation. Because of the highly irregular distribution of data points, which naturally all lie at the perimeters of the basalt outcrops, we have employed a natural neighbor interpolation technique (Sambridge et al. 1995) to minimize model artifacts in the interpolated surface. The resulting map of the subbasaltic surface is shown in figure 8a. Although the interpolation tends to smooth the surface significantly between the basalt peaks, some interesting characteristics do emerge.

The subbasaltic surface shows an approximate 1° northeastward tilt, with maximum elevations of around 1000 m in the west and minimum elevations <750 m in the northeast, constrained by the Mt. Tootie outcrop. The Middle Miocene relief appears to have been significantly lower than the present-day relief. Maximum relief of the subbasaltic surface is ~250 m, whereas the present-day relief in the study area reaches 700 m. The major gorges in the present-day topography are not evident in the Miocene surface. A precursor of the Grose Valley may have existed (recorded by the Mt. Caley basalt) and would have been 100–200 m deep. In contrast, there is no evidence for the existence of the Bowens Creek valley, which nowadays separates Mt. Tomah from Mt. Wilson. We have control on this because of the occurrence of basalt at

constant elevations on buttresses to the south of Mt. Wilson and on Haystack ridge, a line of remnant peaks within the Bowens Creek valley (cf. fig. 4). In general, the Miocene landscape appears to have been characterized by wide, low-relief plateaus separated from each other by broad shallow valleys.

The remarkable contrast between the Middle Miocene and the present-day topography distinguishes the Blue Mountains region from other areas in the southeastern highlands where mapping of subbasaltic surfaces indicated landscape stability during Cenozoic times (e.g., Bishop et al. 1985; Taylor et al. 1985, 1990; Young and McDougall 1993). We explain this contrast as resulting from the passage through our study area of major knickpoints migrating up the river valleys during late Cenozoic times. The present-day Grose River profile gradually and continuously steepens toward the gorge head near its source. However, high-altitude basalts on the gorge sidewalls (Mt. Banks and Mt. Hay outcrops) suggest that the Middle Miocene profile of the Grose River headwaters must have been much gentler and that a major knickpoint must have existed somewhere downstream (fig. 9). Nott et al. (1996), Seidl et al. (1996), and Weissel and Seidl (1998) have recently argued that incision of the

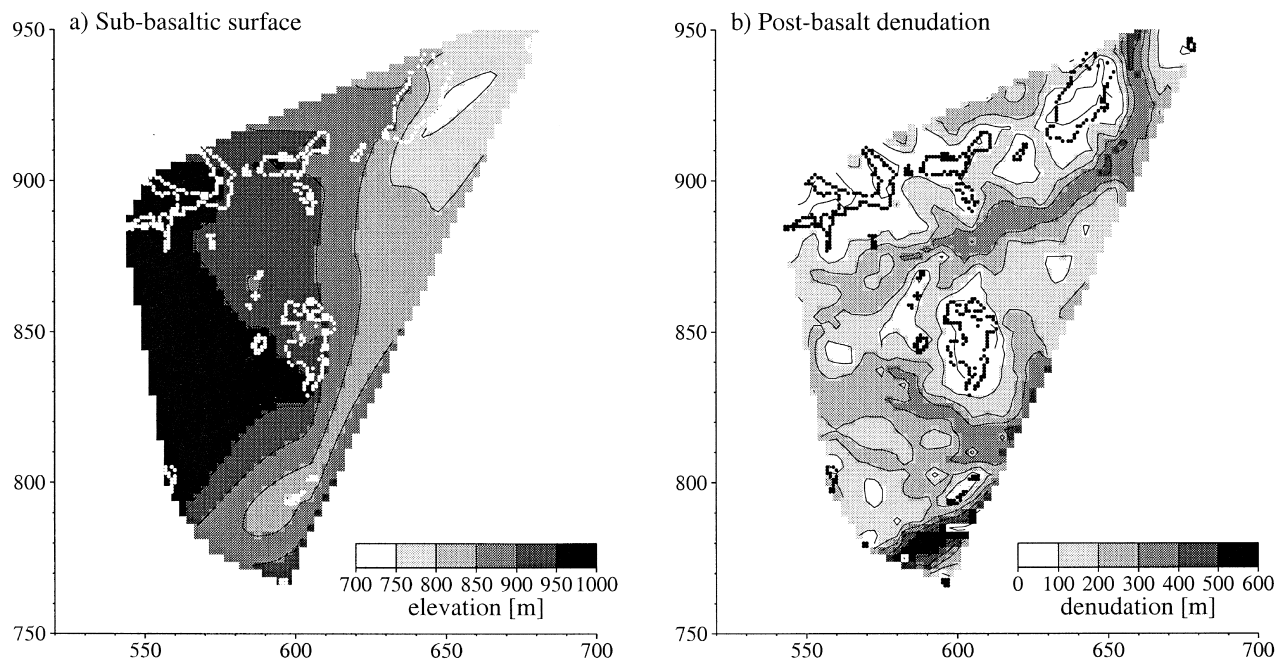


Figure 8. Maps of (a) paleotopography as recorded by the interpolated subbasaltic surface and (b) postbasalt denudation (difference between subbasaltic surface and present-day topography). Data points are indicated by black dots; interpolation has been performed using a natural-neighbor algorithm (Sambridge et al. 1995). See text for discussion.

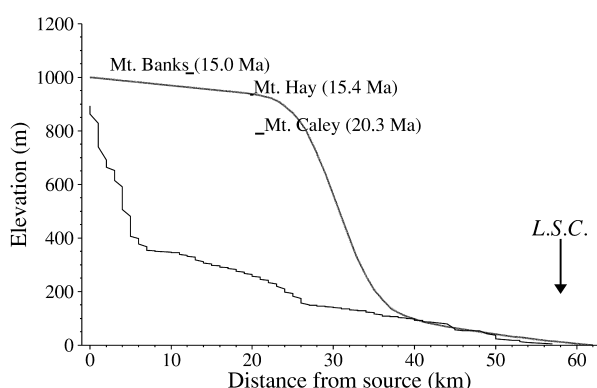


Figure 9. Present-day long profile of the Grose River and projected locations of basalt outcrops on Mts. Banks, Hay, and Caley, indicating maximum depth of paleovalley during the Miocene. A hypothetical mid-late Miocene long profile for the Grose River is indicated by the thick shaded line and highlights the importance of river incision by knickpoint retreat. Annotated arrow indicates location where the Grose River crosses the Laptone Structural Complex (LSC).

southeastern highlands of Australia occurs mainly by knickpoint retreat in river gorges cutting through the escarpment and that this mode of landscape development leads to a dramatic increase in local relief. We suggest a similar evolution for the Blue Mountains region.

Denudation Rates. The comparison of the reconstructed Middle Miocene and present-day topographies provides an estimate of regional denudation rates. Figure 8b shows a map of postbasalt denudation constructed by subtracting the present-day topography from the subbasaltic surface. The map suggests that present-day hilltops and elevated plateaus have had <200 m of material stripped from them since the basalts erupted. In contrast, maximum postbasalt incision reaches 400 m in Bowens Creek and over 600 m in the Grose River gorge. If we assume an age of 15 Ma for the subbasaltic surface, this leads to estimated rates of <14 m m.yr.⁻¹ for upland lowering and ≤40 m m.yr.⁻¹ for river incision. We can compare these estimates to similar ones from other regions of the southeastern highlands (table 2).

The plateau-lowering rates for the Blue Mountains are of roughly the same magnitude as those measured at other localities in the southeastern highlands, as well as with regional-scale estimates of denudation inferred from mass-balance studies and apatite fission-track thermochronology. Fission-track data from large parts of the southeastern Australian highlands (e.g., Gleadow et al. 1996;

O'Sullivan et al. 1996b) suggest long-term denudation rates in the order of 10 m m.yr.⁻¹, consistent with most of the geomorphic and mass-balance estimates (e.g., Bishop 1985; Bishop and Goldrick 1999). Relatively young fission-track ages of ~95 Ma have been encountered in the Bathurst region west of the Blue Mountains (O'Sullivan et al. 1995), as well as in the Snowy Mountains (Kohn et al. 1999), and have been interpreted as representing post-mid-Cretaceous regional denudation rates of up to 40 m m.yr.⁻¹. A few samples from the Blue Mountains region (O'Sullivan et al. 1996a) have yielded large spreads in apparent fission-track ages between ~80 and >200 Ma, interpreted to result from a mixing of provenance ages with ages reset by mid-Cretaceous fluid flow as well as burial heating prior to the removal of 1.5–2.0 km of overburden. These data would imply long-term denudation rates of 20 ± 3 m m.yr.⁻¹, somewhat higher than those found here. Most of this denudation may, however, have occurred during the first 10–20 m.yr. following mid-Cretaceous rifting (van der Beek et al. 1999).

In contrast to the plateau-lowering rates, inferred river-incision rates are very high compared with those estimated, using the same methods, in other parts of the southeastern highlands. The only estimate of river downcutting comparable with ours is that of Young and McDougall (1993) for the Tumut River. The Tumut incises the western flank of the Snowy Mountains, the region of highest elevation and relief in southeastern Australia (van der Beek and Braun 1998), which has probably been tectonically uplifted during the Cenozoic (Kohn et al. 1999). In other southeast Australian rivers that have seen major knickpoints migrate upstream, such as the Snowy or the Shoalhaven, Cenozoic incision rates appear to be 3–10 times lower than in the Grose (Fabel and Finlayson 1992; Nott et al. 1996). On the other hand, Weissel and Seidl (1998) recently presented cosmogenic isotope data from the New England region (northern NSW) that imply short-term ($\leq 10^4$ yr) river-incision rates of >100 m m.yr.⁻¹ on a knickpoint, suggesting that the actual process rates leading to knickpoint retreat are much higher than the long-term averages obtained from geomorphic mapping studies.

The above comparison emphasizes the spatial and temporal variability in Cenozoic denudation rates throughout the southeastern highlands of Australia and serves as a caution against unwarranted extrapolation of data from one region of the highlands to the other.

Rates of Knickpoint Retreat and Initiation of Knickpoints. If we accept the hypothesis that the high

Table 2. Estimates of Denudation Rates for Southeastern Australia

Area	Rate (m m.yr. ⁻¹)	Relevant time span (m.yr.)	Reference
Regional denudation rates:			
Lachlan catchment	4	25–0	Bishop (1985)—MB
	1–3	65–0	Bishop (1985)—MB
	13–47	90–65	Bishop (1985)—MB
Central Highlands	~10	250–0	Gleadow et al. [1996]—FT
Eastern Lachlan Fold Belt	~40	95–0	O'Sullivan et al. (1995)—FT
Snowy Mountains	~40	95–0	Kohn et al. (1999)—FT
Plateau lowering rates:			
Monaro Plateau	3–4	~55–0	Taylor et al. (1990)
Western Snowy Mountains	2–5	21–0	Young and McDougall (1993)
Blue Mountains	<10	15–0	This study
Fluvial incision rates:			
Tumut River	18–30	21–0	Young and McDougall (1993)
Tumbarumba Creek	4–15	21–0	Young and McDougall (1993)
Upper Lachlan River	8	20–0	Bishop et al. (1985)
	3–4	50–20	Bishop (1985)
Snowy River	4	~36–0	Fabel and Finlayson (1992)
Shoalhaven River	13	30–0	Nott et al. (1996)
Bakers Creek (New England)	5–100	.1/.01–0	Weissel and Seidl (1998)—CI
Grose River	≤40	15–0	This study

Note. Methods used to estimate denudation rates based on dated basalt remnants where not indicated, otherwise, MB, mass-balance studies; FT, fission-track thermochronology; CI, cosmogenic isotope dating.

local incision rates in the study area result from the migration of a major knickpoint up the Grose River, we can use the distance between the downstream limits of the basalt outcrops and the present-day gorge head to estimate knickpoint-retreat rates. Using the Mt. Banks, Mt. Hay, and Mt. Caley outcrops, we find knickpoint-retreat rates of 0.8–1.2 km m.yr.⁻¹ since 15–20 Ma (cf. fig. 9). These rates are about twice as slow as estimated knickpoint-retreat rates in basement rocks north and south of the study area (Nott et al. 1996; Seidl et al. 1996). Note, however, that they represent minimum estimates because the Miocene knickpoint may have been located anywhere to the east of the three basalt outcrops.

Large fluvial knickpoints on high-elevation rifted margins have been suggested to form as a result of a major baselevel drop associated with rifting and continental breakup (e.g., Seidl et al. 1996; Weissel and Seidl 1998; van der Beek and Braun 1999). Such a baselevel drop would have occurred at the shelf edge where the border faults of the Tasman Sea basin are located. Since the head of the Grose gorge is located 135 km upstream from the mouth of the Hawkesbury River and the continental shelf offshore the Hawkesbury River mouth is ~50 km wide (Colwell et al. 1993), the Grose knickpoint should have migrated ~185 km upstream since the onset of rifting. If we extrapolate our rates of knickpoint retreat back to this locus of origin, we end up with an age of knickpoint initiation (155–230 Ma) much

older than the estimated initiation of rifting (95–100 Ma; Colwell et al. 1993). This suggests that either knickpoint retreat has slowed down considerably during the evolution of the highlands or that the Blue Mountains knickpoints are controlled by a more local baselevel. In theory, we might expect knickpoint retreat to slow down with time because, as the knickpoint approaches the river source, the river discharges, and therefore its power decreases (Howard et al. 1994; van der Beek and Braun 1999). However, Seidl et al. (1996) and Weissel and Seidl (1998) do not observe any dependence of knickpoint-retreat rates on the drainage basin area for the streams they studied, suggesting that parameters other than river power control these rates. Therefore, a constant retreat rate appears to be a reasonable assumption.

The LSC, which bounds the Blue Mountains to the east, may have been fundamental in controlling regional baselevels. If the LSC represents a passively exhumed Triassic structure, as suggested by Pickett and Bishop (1992), the lithological contrast associated with it (relatively friable Wianamatta Shale to the east of the structure versus resistant sandstones of the Hawkesbury and Narrabeen Groups west of it) may have significantly slowed down knickpoint retreat once the structure was reached. Alternatively, renewed early Tertiary uplift on the LSC, as envisaged by Branagan and Pedram (1990), would induce a baselevel drop, rejuven-

venate river profiles, and initiate knickpoints on the monocline.

The LSC lies 57 km downstream of the gorge head along the Grose River (fig. 9). Extrapolation of our estimated knickpoint-retreat rates suggests that the Grose River knickpoint coincided with the LSC between 48 and 71 Ma, that is, latest Cretaceous-Eocene. Although this is a maximum estimate (because our estimates of retreat rates are minima), the coincidence with the suggested timing of reactivation of the structure (Branagan and Pedram 1990; Schmidt et al. 1995) is striking. We therefore suggest that initiation of the Blue Mountains knickpoints by early Tertiary uplift on the LSC is a distinct possibility. Active Cenozoic uplift on the eastern front of the mountains may be invoked to explain the high relief and high fluvial-incision rates encountered in the Blue Mountains, relative to other localities in the southeastern highlands of Australia.

Lithological and Tectonic Controls on Landform Evolution: A Numerical Simulation

To test our scenario for the morphological evolution of the Blue Mountains and to attempt to discriminate between the two hypotheses for the control (lithological or tectonic) that the LSC has exerted on this evolution, we present results of a numerical surface-processes model. The models we employ are based on the more generic simulations of postbreakup landscape development of the southeastern Australian rifted margin by van der Beek and Braun (1999). We test our models by comparing them with the morphology and drainage patterns (e.g., fig. 1), as well as the stratigraphy of the Sydney Basin (fig. 3).

Numerical Model. We use the CASCADE surface processes model (Braun and Sambridge 1997; van der Beek and Braun 1998, 1999) for our numerical simulations. In this model, a landscape is represented by a large number of randomly distributed grid points connected to each other by Delaunay triangulation. The model landform evolution is controlled by short-range hillslope and long-range fluvial transport (e.g., Kooi and Beaumont 1994). Model equations are summarized in figure 10; for a more extensive description of these, see Braun and Sambridge (1997) and van der Beek and Braun (1998, 1999).

Model parameters that we employ are summarized in table 3. The constraints on these parameters have been discussed in detail by van der Beek and Braun (1998, 1999). For the purpose of this article, we will accept these as representing reason-

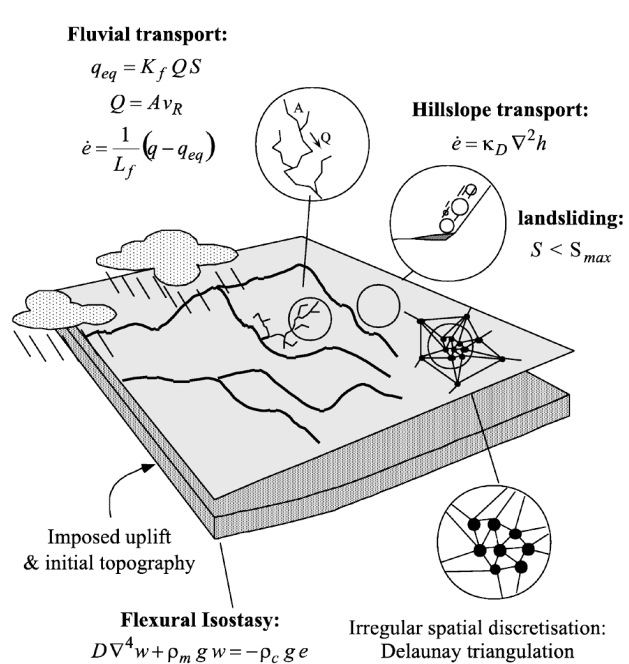


Figure 10. Illustration of CASCADE numerical surface processes model and governing equations (modified from van der Beek et al. 1999). Long-range fluvial incision is controlled by the carrying capacity (q_{eq}) of the rivers, which is controlled by a linear stream power law (Howard et al. 1994) in which K_f is a fluvial transport parameter, Q is discharge (= upstream catchment area $A \times$ precipitation v_R), and S is local river slope. If the carrying capacity of a model river is larger than its actual sediment flux, erosion (e) takes place with a rate determined by the imbalance ($q - q_{eq}$) and a length scale for bedrock incision L_{fb} . If q is larger than q_{eq} , deposition takes place, controlled by a length scale for alluvial deposition L_{fa} . Hillslope processes are modeled by a linear diffusion equation, with κ_D the diffusion coefficient and $\nabla^2 h$ topographic curvature. Mass wasting is modeled by imposing a slope threshold S_{max} ; when this threshold is exceeded, the slope is brought back to it by moving material from the higher grid point toward the lower grid point while conserving mass (van der Beek and Braun 1999). The isostatic response of the lithosphere to denudation (e) is calculated from the deflection (w) of a two-dimensional thin elastic sheet with flexural rigidity D and density ρ_c floating on a mantle with density ρ_m . Parameter values are given in table 3.

able values and we will vary only the initial and boundary conditions of our models to represent the various scenarios we want to test.

Lithological Control Model Simulations. In the first set of models, we adopted Pickett and Bishop's (1992) scenario of landscape development in the

Table 3. Parameter Values for the CASCADE Surface Processes Model

Constraint and symbol	Description	Value
Fitting river profiles and long-term denudation rates: ^{a,b}		
K_f	Fluvial transport parameter	.005
v_R	Precipitation	1 m y ⁻¹
L_{fb}	Length scale for bedrock erosion	300 km; 100 km ^c
L_{fa}	Length scale for alluvial deposition	10 km
Fractal analyses: ^a		
κ_D	Hill-slope diffusion coefficient	.001 m ² y ⁻¹ ; .1 m ² y ⁻¹ ^c
DEM analysis: ^b		
S_{max}	Threshold slope for landsliding	10°
Coherence studies: ^d		
D	Flexural rigidity of the lithosphere	3 × 10 ²² N m

^a van der Beek and Braun 1998.^b van der Beek and Braun 1999.^c The first value is for basement and Narrabeen/Hawkesbury Sandstones; the second for Wianamatta Shale and Permian sediments (see text).^d Zuber et al. 1989.

Blue Mountains in which the LSC is assumed to have been passively exhumed. We show model results for two sets of initial conditions. The first model has an initial topography similar to van der Beek and Braun's (1999) preferred model for the southeastern highlands. In that article, we showed that the "initial" (prebreakup) topography of the highlands provides a fundamental control on their subsequent evolution, and our preferred initial topography included an inland drainage divide that was established at its present location prior to opening of the Tasman Sea. The initial topography in this model consists of a gently seaward-dipping plateau (<1% slope) seaward of the drainage divide (elevation 1000 m) at 130 km from the shoreline; inland the topography slopes down to 600 m at 300 km from the shoreline. During the first 10 m.yr. of the model run, the baselevel at the shoreline is brought down to sea level; the run continues for another 90 m.yr. to model the complete post-breakup evolution of the region.

We embedded the variable lithologies of the Sydney Basin into the model by simplifying the stratigraphy of the basin into three main units: an uppermost easily erodible unit representing the Wianamatta Shale and possible overlying units (now mostly eroded), an intermediate hard unit representing the Hawkesbury and Narrabeen sandstones, and a lower (Permian) unit that is again easily erodible. The middle unit is taken to be 1 km thick and has the same properties as basement (cf. table 3). In contrast, the upper and lower units are characterized by a hillslope diffusion coefficient 100 times higher and a length scale for bedrock incision three times lower than basement. The model Sydney Basin occupies the seaward area (that

is, the first 120 km) of the model. The initial thickness of the upper unit is 1.3 km seaward of the LSC (located between 70 and 80 km inland) and thins from 0.5 to 0 km inland of it. The other units have uniform thickness, but all are offset by 800 m across the monocline.

Results for this model configuration are shown in figure 11. The gross morphology and stratigraphy predicted by this model compare favorably with the observations. The upper soft unit has been nearly completely removed, with only a thin veneer remaining seaward of the LSC. The LSC has formed a secondary escarpment caused by exhumation of the resistant middle unit as envisaged by Pickett and Bishop (1992). Predicted drainage patterns, in contrast, are very different from those observed. The rivers form gorges that incise the part of the basin inland of the LSC, but the predicted drainage pattern is linear and parallel. This is because rivers were established upon an initially seaward-dipping and easily erodible surface; once their courses are entrenched in the landscape, they do not change, even when the rivers start incising into a different lithology.

As an alternative, figure 12 shows a model in which the initial plateau seaward of the (present-day) drainage divide is not inclined but horizontal. Landscape development in such a model is radically different from that in the first one. A drainage-divide escarpment develops at the seaward border of the plateau, and initially, the entire plateau drains inland. However, because the upper unit of the model Sydney Basin is easily erodible, the escarpment retreats rapidly in several (in this case two) embayments, continuously reversing and capturing parts of the inland drainage along the way. This

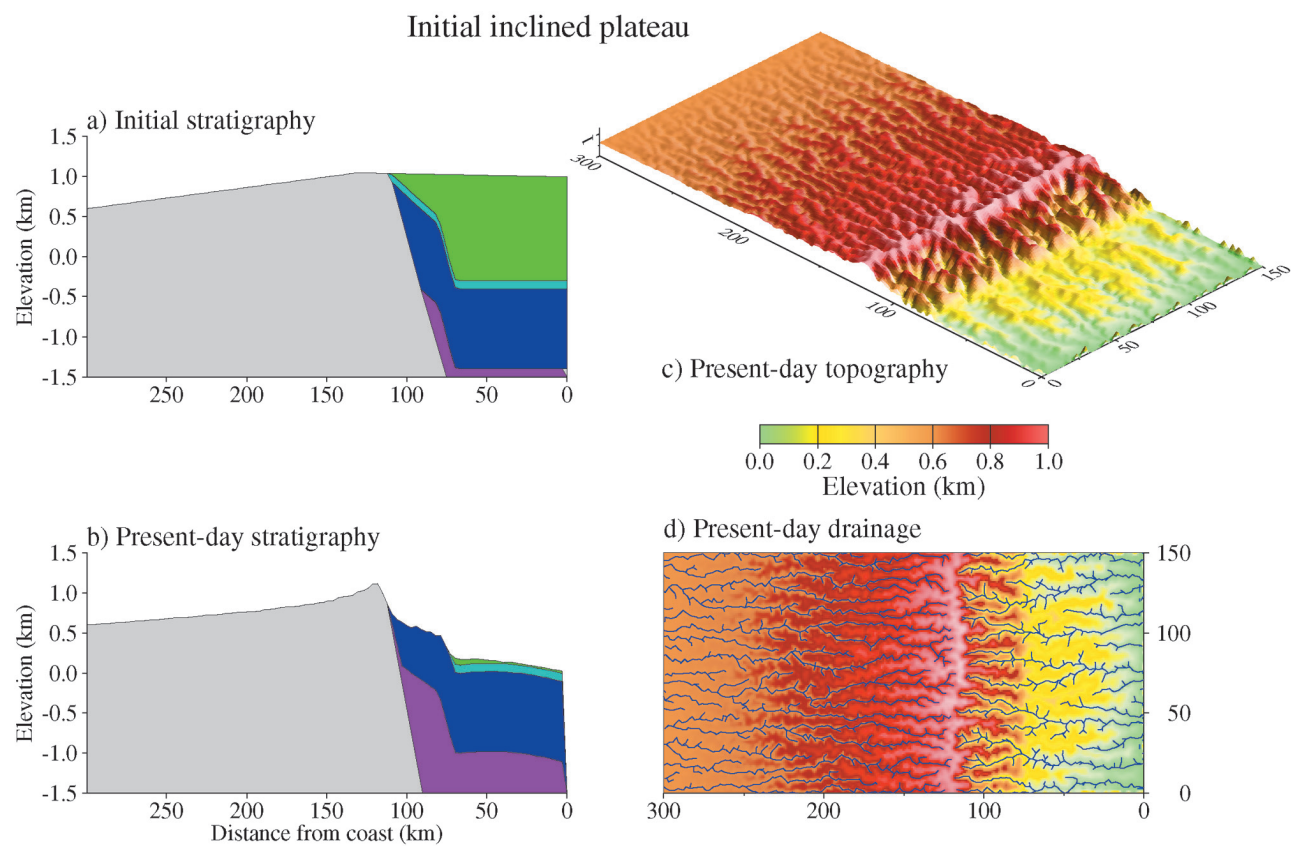


Figure 11. Initial and predicted present-day stratigraphy, topography, and drainage pattern for the model including a preexisting Lapstone Monocline and an initially slightly inclined plateau seaward of a preexisting drainage divide. Initial and predicted present-day stratigraphies (*a* and *b*, respectively) are plotted from a strike-averaged cross section through the models. Stratigraphic units indicated by shading in this and later figures are, from top to bottom, Wianamatta Shale (green), Hawkesbury Sandstone (light blue), Narrabeen Group (dark blue), and Permian units (purple). Distinction between Hawkesbury Sandstone and Narrabeen Group is made solely for visualization purposes. Compare these model predictions with the observed drainage and stratigraphy in figures 1 and 3.

results in a complicated system of gorges draining a plateau region seaward of the retreating drainage divide. The drainage pattern predicted by this model compares more favorably with that observed in the Blue Mountains in that it creates dendritic gorges, but, like the first model, it does not predict drainage to be collected by a major river flowing in front of, and parallel to, the escarpment. The predicted topography and stratigraphy for this model are clearly at odds with the observations. There is much less denudation than in the previous model because the seaward-draining rivers have their headwaters closer to the model edge and thus have less erosive power, although this increases during the model run. Therefore, the model predicts a large wedge of the upper unit still to exist seaward of the LSC, effectively burying the structure so that no

secondary escarpment is formed. Note that the cross section shown in figure 12 is an along strike average between the embayments where the gorges have reached the drainage divide and the central plateau region; it may thus not be very representative of any one section across the model. However, it appears that neither model is able to fully predict the drainage patterns, morphology, and stratigraphy in the Sydney Basin/Blue Mountains.

Tectonic Uplift Model Simulations. In our next model, we test the alternative scenario for landscape development in the Sydney Basin region in which the Blue Mountains plateau was formed by Late Cretaceous–Early Tertiary tectonic uplift along the LSC (Branagan and Pedram 1990; Schmidt et al. 1995). In these models, the initial (prebreakup) morphology of the highlands is a 600-m-high hor-

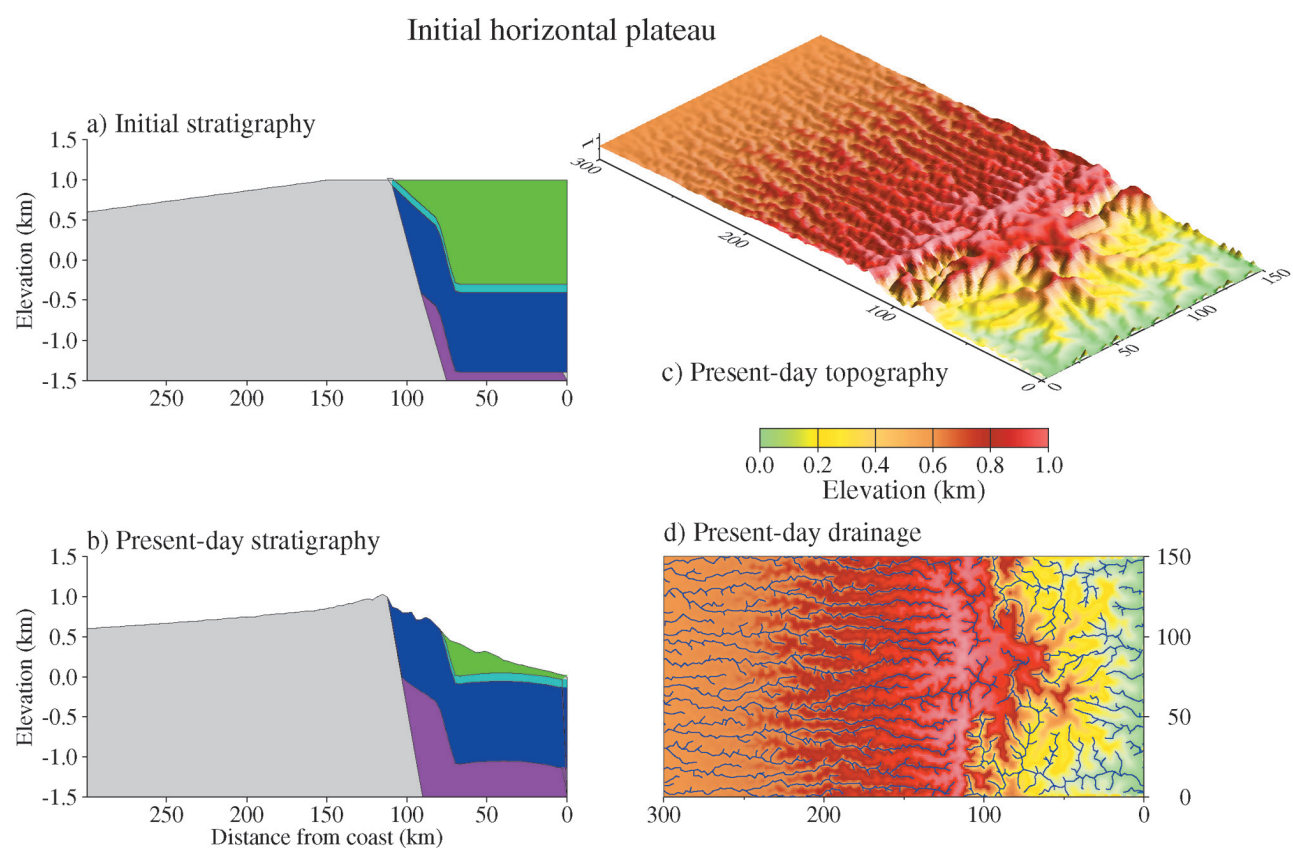


Figure 12. Same as figure 11 but for a model with an initially horizontal seaward plateau

izontal plateau. Between 50 and 40 Ma, uplift takes place, centered on the present-day drainage divide. The drainage divide is uplifted by 800 m, with uplift decreasing to 0 at both sides of the model. The uplift function inland of the drainage divide decreases linearly away from it; seaward of the drainage divide, however, the function is stepped to represent differential uplift on the LSC. We again embed the Sydney Basin in the model; in this case the initial basin has a horizontally layered stratigraphy, and the upper unit is 500 m thick throughout.

The evolution of drainage and morphology in this model is depicted in figure 13. Uplift of the Blue Mountains plateau leads to a major rearrangement of the preexisting inland drainage by diversion of streams seaward of the locus of maximum uplift. These streams are “caught” between the preexisting drainage-divide escarpment and the newly uplifted monocline and develop into a longitudinal river. Finally, the preexisting escarpment is eroded away, and we are left with a river that flows parallel

to the newly formed escarpment, very much analogous to the Nepean River system. We suggest that this is a mechanism by which the remarkable drainage of the Blue Mountains may have formed.

The model predicts the entire upper unit to be eroded away, exposing model Hawkesbury Sandstone in the region seaward of the LSC and Narrabeen Group on the inland plateau. Because the resistant units are exhumed throughout this model, an escarpment forms at the locus of the monocline, and the model Blue Mountains plateau is at an elevation of ~600 m, comparable with the observations. The model predicts a second escarpment to form inland of the model Sydney Basin where Paleozoic basement becomes exposed. This escarpment forms because of the lateral variation in erodibility between the (“soft”) uppermost sediment unit and the (“hard”) basement. The increase in mean elevation across the Blue Mountains is more accentuated in this model than in the actual topography (fig. 14), suggesting that the cover of eas-

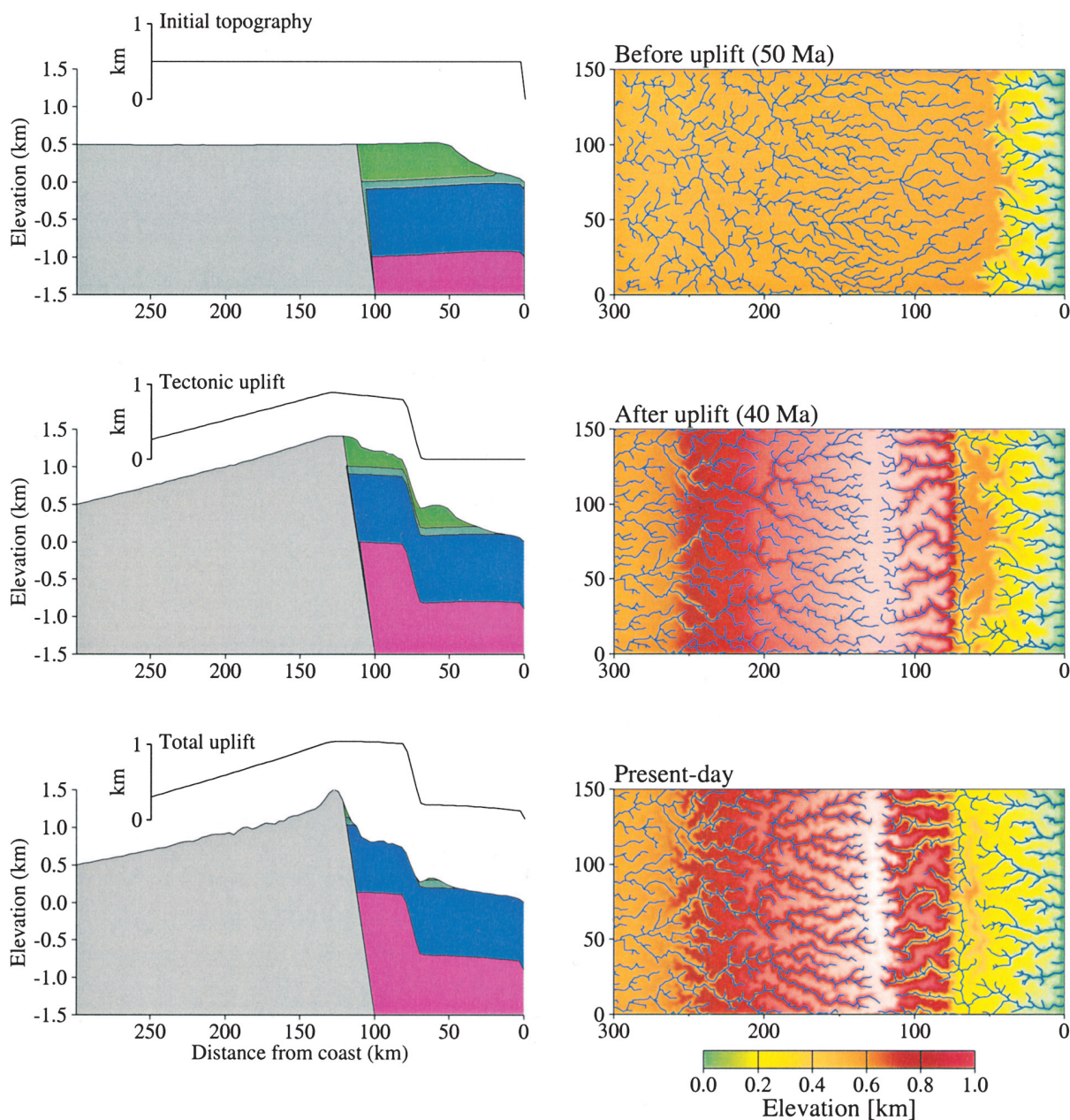


Figure 13. Snapshots of topography, stratigraphy, and drainage at three times during the evolution of the model that includes uplift on the LSC. Insets in cross sections show initial topography at onset of model run, tectonic uplift between 50 and 40 m.yr. ago., and total (tectonic + isostatic) uplift at the end of the model run.

ily erodible material overlying the Blue Mountains plateau must have initially thinned westward.

The observed topography and stratigraphy therefore indicates that the LSC is, at least partly, a pre-existing structure. Our model results suggest, however, that the observed drainage patterns in the Sydney Basin are most easily explained by a model with (renewed) uplift on the LSC.

Discussion and Conclusions

Although many workers have hitherto treated rifted continental margins as essentially two-dimensional structures, our study of landform evolution in the Blue Mountains documents important lateral variations in landform evolution on the southeastern Australian rifted margin. The basalt

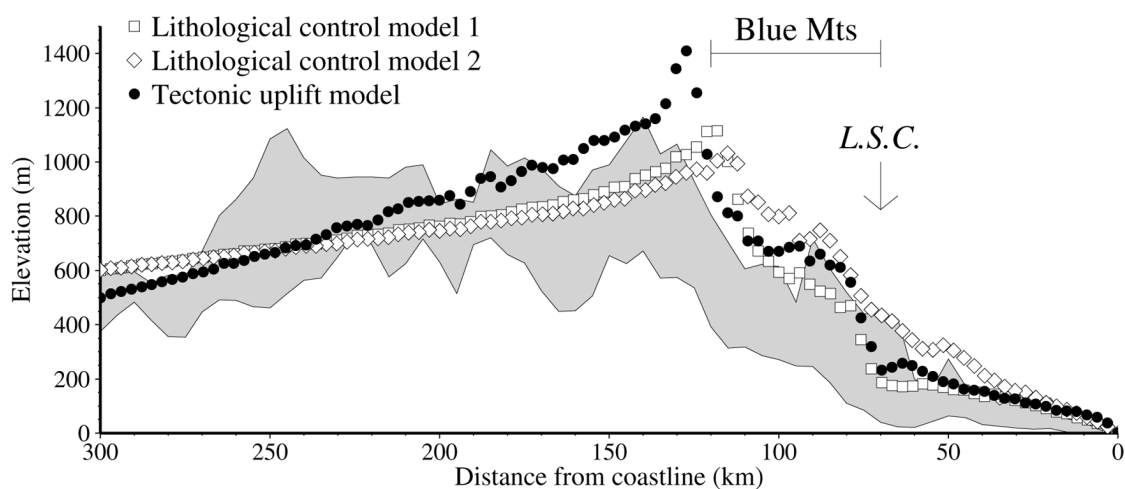


Figure 14. Comparison between observed strike-averaged topography (shaded) in a ~100-km-wide northwest-south-east swath across the Sydney Basin (after van der Beek and Braun 1999) with predictions from the models presented in figures 11–13.

remnants in the Blue Mountains preserve a Middle Miocene landscape of remarkably low local relief. This finding contrasts strongly to studies elsewhere in the southeastern highlands (Bishop et al. 1985; Taylor et al. 1985, 1990; Nott 1992; Young and McDougall 1993) in which similarly aged or older basalts preserve landscapes with a morphology comparable to the present day. Moreover, fluvial-incision rates of up to 40 m m.yr^{-1} , calculated from the vertical distance between the base of the basalts exposed in gorge sidewalls and the present-day riverbed, are 3–10 times higher than those calculated using a similar approach in other localities in southeastern Australia. These results underline the importance of lateral variations in the mode of landscape development and rates of denudation on rifted margins and serve as a caution against uncritical extrapolation of geomorphically derived rates of landscape change outside the immediate study region.

We suggest that the significant Neogene increase in relief in the Blue Mountains is controlled by the migration of major fluvial knickpoints up the river valleys toward the drainage divide where they are now pinned. Our study therefore supports previous results that suggest that knickpoint migration is a fundamental mechanism of landscape development on rifted continental margins (e.g., Gilchrist et al. 1994; Nott et al. 1996; Seidl et al. 1996). However, extrapolation of inferred knickpoint-retreat rates of $0.8\text{--}1.2 \text{ km m.yr}^{-1}$ suggests that the Blue Mountains knickpoints did not originate at the locus of syn-rift baselevel drop (that is, the shelf edge) dur-

ing mid-Cretaceous rifting but rather originated during the latest Cretaceous-Paleogene on the LSC.

Numerical surface process model simulations suggest that both lithological control, resulting from the difference in lithologies exposed east and west of the LSC, as well as renewed early Cenozoic tectonic uplift on it have played a role in shaping the present-day morphology of the Blue Mountains. Contrasting scenarios for the structural evolution of the LSC and the associated morphotectonic evolution of the Blue Mountains (e.g., Branagan and Pedram 1990; Pickett and Bishop 1992) therefore appear to emphasize different aspects of a complex structural and geomorphic history.

The probable early Tertiary tectonic uplift in the Blue Mountains is an important aspect of the post-breakup evolution of the southeastern Australian rifted margin. Such uplift has recently also been invoked for the Snowy Mountains (Kohn et al. 1999) and for parts of the Victorian Alps (Webb et al. 1991; O'Sullivan et al. 1999), whereas other regions within the highlands have been demonstrably stable during the Cenozoic (Bishop et al. 1985; Taylor et al. 1990). Stable regions are characterized by low-relief upland plateaus at around 1000 m elevation, whereas the areas of inferred Cenozoic uplift have much higher mean elevation and relief (van der Beek and Braun 1998). It thus seems that at least part of the lateral variation in morphology of the southeastern Australian rifted margin may be related to localized, fault-bounded early Cenozoic uplift.

Although the evidence for localized postrift uplift

within the southeastern highlands appears mounting, the dynamics of such uplift remain unclear. The present-day stress field in southeastern Australia is compressive, with the σ_1 axis oriented east-west (Lambeck et al. 1984). Although very little data pertaining to the temporal evolution of the stress field are available, the present-day stress regime is generally assumed to have been installed during the Eocene, contemporaneous with the onset of the India-Asia collision and a major change in Pacific plate motion (e.g., Veevers 2000). Major controls on the present-day stress field, apart from far field plate tectonic forces, appear to be exerted by erosional rebound of the highlands and flexural loading of the Tasman Sea margin (Lambeck et al. 1984; Zhang et al. 1998). Denudational rebound appears to drive fault reactivation on the inner margin of the highlands (Bishop and Brown 1992; Goldrick and Bishop 1995) but does not appear to be able to explain kilometer-scale localized uplift within the core of the highlands. Although a link between localized uplift and the evolution of the far field stress regime seems plausible, the uplifts appear to occur along vertical dip-slip basement faults, the reactivation of which is not easily explained in an Andersonian stress system (e.g., Heeremans et al. 1996). Alternatively, the timing of uplift, coeval with the onset of onshore volcanism, as well as its characteristic spacing, suggests that uplift may be related to small-scale mantle diapirism and magmatic underplating (Lister and Etheridge 1989;

Rohrman and van der Beek 1996). The correlation of the areas of maximum uplift with Bouguer gravity minima (Young 1989) may support such a scenario.

ACKNOWLEDGMENTS

This study was performed while P. van der Beek was a postdoctoral fellow and A. Pulford was an honors student at the Research School of Earth Sciences, Australian National University (ANU). We acknowledge Kurt Lambeck for initiating the project, Ian McDougall for guidance in the analysis and interpretation of K-Ar data, and Tony Eggleton for providing access to geochemical facilities at the ANU geology department. We thank John Pickett for his enthusiastic support and for introducing us to the field area. The article benefited from constructive reviews by Ramón Arrowsmith and Paul Bishop. Permission to sample in the Blue Mountains National Park by the New South Wales National Parks and Wildlife Service is acknowledged; we also thank the residents of Mts. Tomah, Wilson, Tootie, and Irvine for access to their properties. The Digital Elevation Model of southeastern Australia was provided by the Australian Surveying and Land Information Group. Natural neighbor interpolation to produce the subbasaltic surface was performed using the nn_quick code (Sambridge et al. 1995). Figures were prepared using GMT software (Wessel and Smith 1998).

REFERENCES CITED

- Bishop, P. 1985. Southeast Australian late Mesozoic and Cenozoic denudation rates: a test for late Tertiary increases in continental denudation. *Geology* 13: 479–482.
- . 1988. The eastern highlands of Australia: the evolution of an intraplate highland belt. *Prog. Phys. Geogr.* 12:159–182.
- Bishop, P., and Brown, R. 1992. Denudational isostatic rebound of intraplate highlands: the Lachlan River valley, Australia. *Earth Surf. Proc. Landf.* 17:345–360.
- Bishop, P., and Goldrick, G. 1999. Geomorphological evolution of the East Australia continental margin. In Summerfield, M. A., ed. *Geomorphology and global tectonics*. Chichester, Wiley, p. 225–254.
- Bishop, P.; Hunt, P.; and Schmidt, P. W. 1982. Limits to the age of the Lapstone Monocline, N.S.W.—a palaeomagnetic study. *J. Geol. Soc. Aust.* 29:319–326.
- Bishop, P.; Young, R. W.; and McDougall, I. 1985. Stream profile change and longterm landscape evolution: Early Miocene and modern rivers of the east Australian highland crest, central New South Wales, Australia. *J. Geol.* 93:455–474.
- Branagan, D. F.; Herbert, C.; and Langford-Smith, T. 1976. An outline of the geology and geomorphology of the Sydney Basin. Sydney, Science Press for the Department of Geology and Geophysics, University of Sydney, 60 pp.
- Branagan, D. F., and Pedram, H. 1990. The Lapstone structural complex, New South Wales. *Aust. J. Earth Sci.* 37:23–36.
- Braun, J., and Sambridge, M. 1997. Modelling landscape evolution on geological time scales: a new method based on irregular spatial discretization. *Basin Res.* 9: 27–52.
- Brown, R. W.; Rust, D. J.; Summerfield, M. A.; Gleadow, A. J. W.; and De Wit, M. C. J. 1990. An Early Cretaceous phase of accelerated erosion on the south-western margin of Africa: evidence from apatite fission track analysis and the offshore sedimentary record. *Nucl. Tracks Radiat. Meas.* 17:339–350.
- Browne, W. R. 1969. Geomorphology—general notes. In

- Packham, G. M., ed. The geology of New South Wales. *J. Geol. Soc. Aust.* 16:559–569.
- Bryan, J. H., ed. 1966. Geological map of Australia, sheet 56-5 (Sydney). N. S. W. Geol. Surv., scale 1 : 250,000.
- Carne, J. E. 1908. Geology and mineral resources of the western coal field. N. S. W. Geol. Surv. Mem. 6:1–246.
- Colwell, J. B.; Coffin, M. F.; and Spencer, R. A. 1993. Structure of the southern New South Wales continental margin, southeastern Australia. *J. Aust. Geol. Geophys.* 13:333–343.
- Davies, P. J. 1975. Shallow seismic structure of the continental shelf, southeast Australia. *J. Geol. Soc. Aust.* 22:345–359.
- Fabel, D., and Finlayson, B. L. 1992. Constraining variability in south-east Australian long-term denudation rates using a combined geomorphological and thermo-chronological approach. *Z. Geomorphol.* 36:293–305.
- Gallagher, K., and Brown, R. W. 1997. The onshore record of passive margin evolution. *J. Geol. Soc. Lond.* 154: 451–457.
- Gallagher, K.; Hawkesworth C. J.; and Mantovani, M. J. M. 1994. The denudation history of the onshore continental margin of southeastern Brazil inferred from apatite fission track data. *J. Geophys. Res.* 99: 18,117–18,145.
- Gilchrist, A. R.; Kooi, H.; and Beaumont, C. 1994. The post-Gondwana geomorphic evolution of southwestern Africa: implications for the controls on landscape development from observations and numerical experiments. *J. Geophys. Res.* 99:12,211–12,228.
- Gilchrist, A. R., and Summerfield, M. A. 1990. Differential denudation and flexural isostasy in formation of rifted-margin upwarps. *Nature* 346:739–742.
- . 1994. Tectonic models of passive margin evolution and their implications for theories of long-term landscape development. In Kirkby, M. J., ed. *Process models and theoretical geomorphology*. New York, Wiley, p. 221–246.
- Gleadow, A. J. W.; Kohn, B. P.; Gallagher, K.; and Cox, S. J. D. 1996. Imaging the thermotectonic evolution of eastern Australia during the Mesozoic from fission track dating of apatites. In *Proceedings, Mesozoic geology of the Eastern Australia plate conference*, Brisbane, September 1996. Geol. Soc. Aust. Ext. Abstr. 43: 195–204.
- Goldberry, R. 1972. Geology of the Western Blue Mountains. N. S. W. Geol. Surv. Bull. 20:1–172.
- Goldrick, G., and Bishop, P. 1995. Differentiating the role of lithology and uplift in the steepening of bedrock river long profiles: an example from southeastern Australia. *J. Geology* 103:227–231.
- Heeremans, M. M. H.; Stel, H.; van der Beek, P. A.; and Lankreijer, A. C. 1996. Tectono-magmatic control on vertical dip-slip basement faulting: an example from the Fennoscandian Shield. *Terra Nova* 8:129–140.
- Howard, A. D.; Dietrich, W. E.; and Seidl, M. A. 1994. Modeling fluvial erosion on regional to continental scales. *J. Geophys. Res.* 99:13,971–13,986.
- Kohn, B. P.; Gleadow, A. J. W.; and Cox, S. J. D. 1999. Denudation history of the Snowy Mountains—evidence from apatite fission track thermochronology. *Aust. J. Earth Sci.* 46:181–198.
- Kooi, H., and Beaumont, C. 1994. Escarpment evolution on high-elevation rifted margins: insights derived from a surface processes model that combines diffusion, advection and reaction. *J. Geophys. Res.* 99: 12,191–12,210.
- Lambeck, K.; McQueen, H. W. S.; Stephenson, R.; and Denham, D. 1984. The state of stress within the Australian continent. *Ann. Geophys.* 2:723–742.
- Lister, G. A., and Etheridge, M. A. 1989. Detachment models for uplift and volcanism in the Eastern Highlands, and their application to the origin of passive margin mountains. In Johnson, R. W., ed. *Intraplate volcanism in Eastern Australia and New Zealand*. Cambridge, Cambridge University Press, p. 297–313.
- Middlemost, E. A. K. 1975. The basalt clan. *Earth Sci. Rev.* 11:337–364.
- Middleton, M. F. 1993. Thermo-tectonic influences on the Sydney Basin during the breakup of Gondwana. In Findlay, R. H.; Unrug, R.; Banks, M. R.; and Veevers, J. J., eds. *Gondwana eight: assembly, evolution and dispersal*. Rotterdam, Balkema, p. 613–622.
- Nott, J. F. 1992. Long-term drainage evolution in the Shoalhaven catchment, southeast highlands, Australia. *Earth Surf. Proc. Landf.* 17:361–374.
- Nott, J. F.; Young, R. W.; and McDougall, I. 1996. Wearing down, wearing back and gorge extension in the long-term evolution of a highland mass: quantitative evidence from the Shoalhaven catchment, southeast Australia. *J. Geol.* 104:224–232.
- Ollier, C. D. 1982. The Great Escarpment of eastern Australia: tectonic and geomorphic significance. *J. Geol. Soc. Aust.* 29:13–23.
- O'Sullivan, P. B.; Coyle, D. A.; Gleadow, A. J. W.; and Kohn, B. P. 1996a. Late Mesozoic to Early Cenozoic thermotectonic history of the Sydney Basin and the eastern Lachlan fold belt, Australia. In *Proceedings Mesozoic geology of the Eastern Australia plate conference*, Brisbane, September 1996. Geol. Soc. Aust. Ext. Abstr. 43:424–432.
- O'Sullivan, P. B.; Foster, D. A.; Kohn, B. P.; and Gleadow, A. J. W. 1996b. Multiple post-orogenic denudation events: an example from the eastern Lachlan Fold Belt, Australia. *Geology* 24:563–566.
- O'Sullivan, P. B.; Kohn, B. P.; Foster, D. A.; and Gleadow, A. J. W. 1995. Fission track data from the Bathurst Batholith: evidence for rapid mid-Cretaceous uplift and erosion within the eastern highlands of Australia. *Aust. J. Earth Sci.* 42:597–607.
- O'Sullivan, P. B.; Orr, M.; O'Sullivan, A. J.; and Gleadow, A. J. W. 1999. Episodic Late Palaeozoic to recent denudation of the Eastern Highlands of Australia: evidence from the Bogong High Plains, Victoria. *Aust. J. Earth Sci.* 46:199–216.
- Pickett, J. 1984. Pre-basalt topography on Mount Tomah, New South Wales. N. S. W. Geol. Surv. Quart. Notes 57:22–27.
- Pickett, J., and Bishop, P. 1992. Aspects of landscape evo-

- lution in the Lapstone Monocline area, New South Wales. *Aust. J. Earth Sci.* 39:21–28.
- Pulford, A. 1997. Cenozoic landscape evolution of the east Australian highlands: constraints from Miocene basalts, Blue Mountains, N. S. W. Unpub. Honors thesis, Australian National University, Canberra, 86 p.
- Rohrman, M., and van der Beek, P. A. 1996. Cenozoic post-rift uplift of North Atlantic margins: an asthenospheric diapirism model. *Geology* 24:901–904.
- Sambridge, M.; Braun, J.; and McQueen, H. 1995. Geophysical parameterization and interpolation of irregular data using natural neighbours. *Geophys. J. Int.* 122:837–857.
- Schmidt, P. W.; Lackie, M. A.; and Anderson, J. C. 1995. Palaeomagnetic evidence for the age of the Lapstone Monocline, N.S.W. *Aust. Coal Geol.* 10:14–19.
- Seidl, M. A.; Weissel, J. K.; and Pratson, L. F. 1996. The kinematics and pattern of escarpment retreat across the rifted continental margin of SE Australia. *Basin Res.* 8:301–316.
- Steiger, R. H., and Jäger, E. 1977. Subcommission on geo-chronology: convention on the use of decay constants in geo- and cosmochronology. *Earth Planet. Sci. Lett.* 36:359–362.
- Summerfield, M. A. 1991. Global geomorphology. Harlow, Longman, 537 p.
- Taylor, G.; Taylor, G. R.; Bink, M.; Foudoulis, C.; Gordon, I.; Hedstrom, J.; Minello, J.; and Whippy, F. 1985. Pre-basaltic topography of the Northern Monaro and its implications. *Aust. J. Earth Sci.* 32:65–71.
- Taylor, G.; Truswell, E. M.; McQueen, K. G.; and Brown, M. C. 1990. Early Tertiary palaeogeography, landform evolution, and palaeoclimates of the Southern Monaro, N.S.W., Australia. *Palaeogeogr. Palaeoclimatol. Palaeoecol.* 78:109–134.
- van Balen, R. T.; van der Beek, P. A.; and Cloetingh, S. 1995. The effect of rift shoulder erosion on stratigraphic patterns at passive margins: implications for sequence stratigraphy. *Earth Plan. Sci. Lett.* 134: 527–544.
- van der Beek, P. A.; Andriessen, P. A. M.; and Cloetingh, S. 1995. Morphotectonic evolution of rifted continental margins: inferences from a coupled tectonic-surface processes model and fission track thermochronology. *Tectonics* 14:406–421.
- van der Beek, P. A., and Braun, J. 1998. Numerical modelling of landscape evolution on geological time-scales: a parameter analysis and comparison with the southeastern highlands of Australia. *Basin Res.* 10: 49–68.
- . 1999. Controls on post-mid-Cretaceous landscape evolution in the southeastern highlands of Australia: insights from numerical surface process models. *J. Geophys. Res.* 104:4945–4966.
- van der Beek, P. A.; Braun, J.; and Lambeck, K. 1999. The post-palaeozoic uplift history of southeastern Australia revisited: results from a process-based model of landscape evolution. *Aust. J. Earth Sci.* 46:157–172.
- Veevers, J. J. 2000. Change of tectono-stratigraphic regime in the Australian plate during the 99 Ma (mid-Cretaceous) and 43 Ma (mid-Eocene) swerves of the Pacific. *Geology* 28:47–50.
- Veevers, J. J.; Conaghan, P. J.; and Powell, C. M. 1994. Eastern Australia. In Veevers, J. J., and Powell, C. M., eds. Permian-Triassic Pangean basins and foldbelts along the Panthalassan margin of Gondwanaland. *Geol. Soc. Am. Mem.* 184:11–171.
- Webb, J. A.; Finlayson, B. L.; Fabel, D.; and Ellaway, M. 1991. The geomorphology of the Buchan Karst—implications for the landscape history of the Southeastern Highlands of Australia. In Williams, M. A. J.; De Deckker, P.; and Kershaw, A. P., eds. *The Cainozoic in Australia: a re-appraisal of the evidence*. Geol. Soc. Aust. Spec. Publ. 18:210–234.
- Weissel, J. K., and Seidl, M. A. 1998. Inland propagation of erosional escarpments and river profile evolution across the southeast Australian passive continental margin. In Tinkler, K. J., and Wohl, E. E., eds. *Rivers over rock: fluvial processes in bedrock channels*. Am. Geophys. Union Monogr. 107:189–206.
- Wellman, P. 1979. On the Cainozoic uplift of the southeastern Australian highland. *J. Geol. Soc. Aust.* 26: 1–9.
- Wellman, P., and McDougall, I. 1974. Potassium-Argon ages on the Cainozoic volcanic rocks of New South Wales. *J. Geol. Soc. Aust.* 21:247–272.
- Wessel, P., and Smith, W. H. F. 1998. New, improved version of the Generic Mapping Tools Released. *EOS Trans. Am. Geophys. Union* 79:579.
- Wilson, M. 1989. Igneous petrogenesis. London, Harper Collins Academic, 466 p.
- Young, R. W. 1983. The tempo of geomorphological change: evidence from southeastern Australia. *J. Geol.* 91:221–230.
- . 1989. Crustal constraints on the evolution of the continental divide of eastern Australia. *Geology* 17: 528–530.
- Young, R. W., and McDougall, I. 1985. The age, extent and geomorphological significance of the Sassafras basalt, southeastern New South Wales. *Aust. J. Earth Sci.* 32:323–331.
- . 1993. Long-term landscape evolution: Early Miocene and modern rivers in southern New South Wales, Australia. *J. Geol.* 101:35–49.
- Young, R. W., and Nanson, G. C., eds. 1983. Aspects of Australian sandstone landscapes. Aust. N. Z. Geomorph. Group Spec. Publ. 1, 126 p.
- Zhang, Y.; Scheibner, E.; Hobbs, B. E.; Ord, A.; Drummond, B. J.; and Cox, S. J. D. 1998. Lithospheric structure in southeast Australia: a model based on gravity, geoid and mechanical analyses. In Braun, J.; Dooley, J.; Goleby, B.; van der Hilst, R.; and Klootwijk, C., eds. *Structure and evolution of the Australian continent. Geodynamics Series*. Washington, D.C., Am. Geophys. Union.
- Zuber, M. T.; Bechtel, T. D.; and Forsyth, D. W. 1989. Effective elastic thickness of the lithosphere and mechanisms of isostatic compensation in Australia. *J. Geophys. Res.* 94:9353–9367.